Response to Reviewer #1's comments on the paper entitled " Atmospheric salt deposition in a tropical mountain rain forest at the eastern Andean slopes of South Ecuador – Pacific or Atlantic origin?"

Please find below our response to the comments of referee #1. Please note that "C" stands for comment and "A" for answer.

General comments:

C: The manuscript discusses the possible source regions affecting sea salt deposition in a tropical mountain rain forest site in Southern Ecuador. The discussion was based on five years of rain and occult precipitation water ion composition data, sea salt aerosol concentration data from MACC (Monitoring Atmospheric Composition and Climate) re-analysis and NOAA/Hysplit backtrajectories. The authors discuss well the contribution of Pacific and Atlantic source areas of NaCl to the study area, combining MACC and backtrajectories datasets. However, both are reanalysis datasets, which are based on satellite, surface observations (scarce in the Amazonian region) and modelling. The link to actual measurements (rain and occult precipitation data) is rather weak, and should be reinforced.

A: Thank you very much for your positive general comment on the manuscript. As the reviewer stressed in comment 12, it is likely that the link between the reanalysis data and the measurements has not been explained clearly enough in the text. The link of both data sets was tested by cross correlation analysis between the MACC sea-salt concentration at different pressure levels and the sodium and chloride concentration measured on the ground. Only after confirming the suitability of the MACC concentration data and selecting the pressure level with the stronger and most significant correlation coefficients, we used it as sea-salt concentration proxy for trajectory modeling. As suggested by the reviewer, the table with the cross correlation coefficients that was included in the appendices has been moved to the data and methods section, to make the relationship between both data sets more explicit and clear. Accordingly, the manuscript has been edited to clarify the connection between modeling and measurement data.

Specific comments:

1) C: The term "salt" is not precise (title and abstract). Better to use "sea salt" instead.
   A: We have considered this recommendation.

2) C: Lines 45-49: references are missing. I suggest Talbot et al., 1990.
   A: we have added these references.

3) C: Line 135: detection limits of cations and anions analysis should be mentioned.
   A: the detection limits have been added to the in the text.

4) C: The rain water data set presented in the manuscript spans from 2004 to 2009. Was part of this dataset published by Fabian et al., 2009? If so, that could be mentioned somewhere.

A: Yes you are right, part of this data set was published in Fabian et. al., 2009. His work is cited in page 5, line 137.

5) C: Section 3.1: the horizontal resolution of MACC reanalysis data should be mentioned: 80 km (Inness et al., 2013).

A: The horizontal resolution of the MACC dataset is now included in the revised manuscript.

6) C: Section 3.2: the frequency of calculated trajectories should be mentioned. Based on the number of trajectories mentioned in the abstract, one could guess that daily trajectories were used. Nevertheless, this should be explicit in the methods section.

A: Yes, we used daily trajectories. This information is now included in the text.

7) C: Section 3.2: Which criteria did you use to define the number of trajectory clusters?

A: We used a partitioning algorithm based on k-Means to define the appropriate number of trajectory clusters. In this context we used prior knowledge of the main wind systems affecting the receptor site. We tested different k values and chose the maximum number of clusters that most successfully reproduced the known conditions. These information has also been incorporated in the revised manuscript.

8) C: Line 224: The authors shall raise hypothesis to explain why Cl- concentrations were usually higher than Na+ in rainwater. Pauliquevis et al., 2012 also reported higher Cl- in Amazonian rainwater. On the other hand, in the aerosol phase, the literature shows Cl/Na molar ratios smaller than 1 in Amazonia (Martin et al., 2010; Junior et al., 2015). Please comment on that.

A: The Cl– concentration was especially higher at the valley meteorological station ECSF and not only for rain but also for OP, so we hypothesized that some of the deposited Cl- could have its origin in Cl-bearing minerals from the street connecting the cities of Loja and Zamora. As we move upslope to the uppermost measurement stations the Na/Cl molar ratio gets very close to the sea water ratio (0.86), especially in OP samples, thus leading to the conclusion that the aerosols at these high altitude sites are predominantly of marine origin. Following the findings of Junior et. Al (2015) in the central Amazon, we cannot rule out other sources for the non-sea water salt at the lower altitude sites as emissions from fertilizers used in the pasture areas and biomass burning in the southern slopes of the valley. However, since in the South Ecuadorian Andes there is no intensive and mechanized agricultural exploitation as in central Brazil, we could expect significantly weaker emissions from these activities. Biomass burning is also a common practice in the region, and Cl- is emitted in relevant quantities in smoke from vegetation fires, so biomass burning emissions probably have an impact. However, the results from factor analysis of ion concentrations from our

field measurements do not corroborate this assumption.

9) C: Lines 240-260 (linked to the previous comment): Figure 3 shows that in some cases Cl- is associated with SO42-, NO3- and K+. In addition to sea spray, are there other sources that could contribute to Cl- in rainwater and OP?
A: This question has been answered in the previous point.

10) C: Table 1 and lines 299-300: please clarify how the percentage of total concentration was calculated.
A: We calculated the sum of the concentration related to the trajectories belonging to each cluster, multiplied it by 100 and then divided by the total concentration in the observation period.

11) C: Table 2 was not discussed, and there is not even a reference to it in the manuscript.
A: Table 2 is referenced and discussed in lines 470-475 in the submitted manuscript. There was a typesetting error in the reference. Table 2 is now table 4 in the revised manuscript.

12) C: Table A1 should not be in the appendix, because it is the only link between actual measurements and MACC reanalysis data. The table caption is not clear. Are the numbers reported the linear correlation coefficient in each case? How about the "mean" column, what is the meaning, and what are the units?
A: We agree with the reviewer's comment. The table has been moved to the data and methods section in the revised manuscript (Table 1). Yes, the numbers are linear correlation coefficients and the mean column shows the correlation coefficients for Na+ and Cl- mean concentration.

13) C: Lines 274-275: I am not convinced that MACC NaCl aerosol concentrations represent well the conditions observed at the ground measurement sites. MACC's horizontal resolution is 80 km, while the distance between the Reserva Biologica San Francisco and the Pacific Ocean is about 100 km. The topography and its significant influence on atmospheric circulation and on the transport of scalars cannot be correctly described within MACC's horizontal resolution. This limitation should be mentioned in the manuscript, as well as the possible bias resulting from that.
A: We tested the applicability of MACC sea-salt concentration by a correlation analysis summarized in table A1 (table 1 in the revised manuscript). Regarding the spatial resolution and its limitations, they have been included in the revised manuscript.

14) C: The results from trajectory cluster analysis, PSCF and CWT are interesting and consistent with each other. However, they are all based on MACC's sea salt particle concentrations, and not on actual measurements. With that, you can only demonstrate that the model within MACC predicts that ~80% of sea salt particles, in a 80 km square area in Ecuador, comes from the Atlantic, and that ~20% comes from the Pacific. To provide stronger evidences, you should include the five years of rain water and occult precipitation observations in the cluster,

PSCF and CWT analysis.

A: We agree with the reviewer and we have adjusted our results and conclusions accordingly.

15) C: In years of El Niño, the Eastern winds typically weaken. Did you notice any trends on sea salt transport in El Niño years between 2004 and 2009?

A: We looked into the relation between the ENSO cycle and the atmospheric transport situation. However, in the study period, no significant El Niño event occurred. Furthermore, the impact of the ENSO cycle in the study area is weak, because it is situated between the both branches of the Walker-cells (Pacific and Amazonian) and a reversal of circulation does not cause much change in precipitation and general wind direction there.

Technical corrections

All the technical recommendations made by the reviewer have been considered.

Response to Reviewer #2's comments on the paper entitled " Atmospheric salt deposition in a tropical mountain rain forest at the eastern Andean slopes of South Ecuador – Pacific or Atlantic origin?"

Please find below our response to the comments of referee #2. Please note that "C" stands for comment and "A" for answer.

General comments:

C: This paper is on an interesting topic that quite frankly I have not thought of before- namely the role that sea spray may have in geochemical cycles and how specifically Na and Cl may be important. In this regard, I think the paper is certainly appropriate for ACP. This said, while I generally get the general idea of what they were doing the paper does not follow traditional lines of analysis from an aerosol point of view. This is not too surprising given the authors background is geography and land surface. But, I would strongly encourage the authors to reach out some colleagues in Germany for some help in interpreting MACC and trajectory analyses. For example, the Max Planck Institute for Chemistry, Mainz is world renowned for their aerosol work in South America and would be worth consulting. I think the authors have something quite interesting right here, but as an aerosol scientist it does not close as neatly as it should for ACP. I thus recommend major revisions with the understanding that they will get some aerosol help.

A: Thank you very much for your constructive comments on the manuscript. We have included additional datasets (ERA-Interim; NOx fluxes caused by biomass burning) and adapted the methodology. We have extended the manuscript according to the new results. Our approach follows the methodology initiated by the work of the late Peter Fabian from TUM Weihenstephan, an expert in atmospheric chemistry who also maintained intensive contacts in the aerosol community including the MPI for chemistry in Mainz. Due to the many papers following traditional approaches we are doing the analyses with a slightly different attitude.

Specific comments:

I am not going to go into details, but I do have several important comments that need to be addressed.

1) C: I am not sure HYSPLIT at 2.5x2.5 degree resolution is a trajectory model of choice for this kind of mountainous terrain. Now this said, it would probably give you the prevailing wind direction (coming from the west or east), but as I think there is some danger of confounders (see next comment) something a bit more sophisticated is in order. Consider, often at altitude you could have easterlies, but coming up the mountains on the westerly side are upslope anabatic winds. This could be an even bigger part of the budget. See comment 3.

A: You are right. In the revised manuscript we have generated new back-trajectories based on wind fields from ERA interim reanalysis, which have a higher spatial resolution. Because of the finer spatial resolution of this data set the topographical effect of the Andes was more realistically represented by the new back-trajectories. Therefore we have replaced the NCEP/NCAR trajectories by ERA Interim trajectories in the revised manuscript.
Regarding the role of the anabatic winds, a new analysis based on wind direction from our ground measurement stations that addresses this question has been added (Fig. 4 in the revised manuscript).

2) C: The authors already noted that biomass burning tracers appeared seasonally in their analysis, and suggest that this corroborated colinear transport of sea salt and biomass burning. Although, they note that Cl is in fact emitted. Actually, Na and Cl are both strongly emitted by biomass burning, and in the July through October time frame, copious amounts of smoke are transported directly over the study region. It has even been noted as a pathway of cloud condensation nuclei in the Central Pacific. In the winter months, smoke from northern South America is also frequently in the region. At the very least biomass burning in MACC should be included in the analysis. Perhaps seasonal maps of total mass load for sea salt and smoke are in order too?

A: Thank you very much for arising this point. As you suggested, we have included new data (MACC NOx fluxes caused by biomass burning) and analysis regarding the potential role of biomass-burning emissions on the sodium and chloride transport over South America.
To look for sea salt sources and sinks along different transport pathways we have extracted the sea salt concentration from the MACC dataset along the cluster mean back trajectories for each season (Fig. 7). Seasonal maps of sea salt and biomass-burning NOx fluxes were calculated which support the spatial interpretation of sodium and chloride sources along the transport pathways (Fig. 8 and 9).

3) C: The authors look at elemental masses, but really they need to look also at molar stoichiometry in this circumstance. Although the paper says that the mass ratio of Cl:Na goes down in time, they need to understand that Cl depletion is in some ways a photochemical clock. If Na:Cl is what it is for fresh sea water, you know it is local-maybe upslope winds. As it goes up, the sea salt is older (across the continent?). This should be included in the analysis

A: We have added new analysis with regard to the Na/Cl molar ratio in rain and occult precipitation (OP). As you mentioned this ratio changes as a function of distance from the coast and is a good indicator of the origin of sodium and chloride concentration in precipitation. Time-series of this ratio were generated for each meteorological station along the altitudinal gradient studied. Likewise, we calculated the ratio at each meteorological station for the total period analyzed (2004-2009). Please see Fig. 3 in the revised manuscript.

4) C:The paper gets in the way of itself in its diction and grammar, and thus a good edit might be in order. Also the way some of the data is presented the data gets to be difficult to interpret. I would then do a time series plot of the factor loadings. In Figure 3 for example, the PCA analysis would be better interpreted as a table. I also had a hard time making heads or tails of the lower figures in figures 4 through 6.
Hope this helps, Jeffrey S. Reid, US Naval Research Laboratory.

A: The language has been edited by a native speaker and the figures changed according to your comments.
Factor analysis plots in the previous version have been replaced by a table showing the factor loadings (Table 2). It is true that as a table the results of this analysis can be better interpreted. Thank you.
The figures in the submitted manuscript have been all edited or replaced by new figures in the revised manuscript, except for figure 1. Following the comments of Dr. Reid, figures 4 through 6 have been removed from the manuscript.

Once again the authors thank Dr. Reid for his valuable comments on the manuscript.

Manuscript prepared for Atmos. Chem. Phys.
with version 2015/04/24 7.83 Copernicus papers of the LaTeX class copernicus.cls.
Date: 8 June 2016

Atmospheric salt deposition in a tropical mountain rain forest at the eastern Andean slopes of South Ecuador - Pacific or Atlantic origin?

Sandro Makowski Giannoni[1], Katja Trachte[1], Ruetger Rollenbeck[1], Lukas Lehnert[1], Julia Fuchs[2], and Joerg Bendix[1]

[1]Laboratory for Climatology and Remote Sensing (LCRS), Institue of Physical Geography, Department of Geography, Philipps-Universitaet, Marburg, Germany
[2]Laboratory of Climatology, Institute of Physical Geography, Department of Geography, Ruhr-Universitaet, Bochum, Germany

Correspondence to: Sandro Makowski Giannoni (sandro.makowski@posteo.org)

Abstract. ~~Salt~~ Sea salt (NaCl) ~~is recently~~ has recently been proven to be of ~~highest~~ the utmost importance for ecosystem functioning ~~of the~~ in Amazon lowland forests because of its ~~importance for~~ impact on herbivory, litter decomposition and, thus, carbon cycling. ~~Salt~~ Sea salt deposition should generally decline ~~with~~ as distance from its marine ~~sources. For tropical South America~~source increases. For the Amazon, a negative east-west ~~salt availability gradient is assumed in the Amazon~~ gradient of sea salt availability is assumed as a consequence of the barrier effect of the Andes Mountains for Pacific air masses. However, this generalized pattern may not hold for the tropical mountain rain forest in the Andes of southern Ecuador. To analyze sea salt availability, we ~~investigate~~ investigated the deposition of sodium (Na^+ ~~and~~) and chloride(Cl^-), which are good proxies of sea spray aerosol. Because of the complexity of the terrain and related cloud and rain formation processes, sea salt deposition was analyzed from both, rain and occult precipitation (OP) ~~water~~ along an altitudinal gradient over a period ~~from~~ between 2004 ~~to~~ and 2009. To assess the influence of ~~Atlantic and Pacific~~ easterly and westerly air masses on the ~~locally observed~~ deposition of sodium and chloride ~~, sea-salt~~ over southern Ecuador, sea salt aerosol concentration data from the Monitoring Atmospheric Composition and Climate (MACC) reanalysis dataset and back-trajectory statistical methods were combined. Our results, based on deposition time series~~and 2192 generated trajectories~~ , show a clear difference in the temporal variation of sodium and chloride concentration ~~due~~ and Na^+/Cl^- ratio in relation to height and exposure to winds. ~~The sea-salt transport was highly seasonal where higher locations revealed a stronger seasonality~~ At higher elevations, sodium and chloride present a higher seasonality and the Na^+/Cl^- ratio is closer to that of sea salt. Medium to long-range sea salt transport exhibited a similar seasonality, which shows the link between our measurements at high elevations and the sea salt synoptic transport. Although the influence of the ~~easterlies~~ Easterlies were predominant regarding the atmospheric circulation, the statistical analysis of trajectories and hybrid receptor models revealed a stronger impact of the

Pacific sea-salt north-equatorial Atlantic, Caribbean, and Pacific sea salt sources on the deposition at the study areaatmospheric sea salt concentration in southern Ecuador. The highest concentration in rain and cloud water was found between September and February originating from both, the equatorial Pacific and Atlantic. However, the Pacific sources contributed with up to 25to the observed total concentration of Na^+ and Cl^- at the receptor site although the frequency of occurrence of the respective trajectories is below 10when air masses originated from the north-equatorial Atlantic, the Caribbean Sea and the equatorial Pacific. Together, these sources accounted for around 82.4% . This highlights the great importance of westerly winds from the Pacific for the sea-salt transport to the deposition into the tropical mountain forests at the eastern Andean slopes of of the sea salt budget over southern Ecuador.

1 Introduction

Poor substrate and intense leaching by precipitation make tropical forests particularly prone to nutrient limitationdeficiency. While phosphorus is mainly claimed to limit considered a limitation to net primary productivity (NPP) in lowland Amazonian tropical forestforests, phosphorus and nitrogen co-limits co-limit growth in the tropical montain rain forestsas e.g mountain rain forests, as in southern Ecuador (Homeier et al., 2012; Koehler et al., 2009; Tanner et al., 1998; Vitousek, 1984; Wolf et al., 2011; Wullaert et al., 2010). Because of a world wide worldwide increase in nitrogen and phosphorus emissions and a particularly accelerated enhancement of emissions in pronounced increase in emissions from developing countries, where most of the the majority of tropical forests are located, atmospheric deposition in these countries has gained some attention (Dentener et al., 2006; Galloway et al., 2008; Phoenix et al., 2006).

Nitrogen and phosphorus cycling and deposition from atmospheric sources are been investigated in In several tropical and temperate forests, where the changes in human intervention in the nitrogen and phosphorus cycles have has been documented (Mahowald et al., 2005; Matson et al., 2002; Phoenix et al., 2006; Tipping et al., 2014; Yu et al., 2015). Because nutrient availability regulates ecosystem processes and functions, the changes currently affecting the nitrogen and phosphorus budgets are expected to have impacts in wide-reaching impacts in forest ecosystem structure and functioning and plant diversity . diversity (Bobbink et al., 2010; Homeier et al., 2012; Matson et al., 2014; Peñuelas et al., 2013; Pett-Ridge, 2009; Wang et al., 2014; Wilcke et al., 2013). The role of sea salt availability has very recently gained attention as it has been found to condition the behaviour behavior of herbivores, as well as in addition to affecting carbon cycling and organic matter decomposition in tropical ecosystems (Dudley et al., 2012; Kaspari et al., 2008, 2009; Powell et al., 2009; Voigt et al., 2008). In spite of At the western rim of the Amazon forest, in Peru, Ecuador, and Colombia, there is evidence that herbivorous and frugivorous birds and mammals visit mineral licks to compensate for low sodium concentration in plant and fruit tissues (Lee et al., 2009; Lizcano and Cavelier,

2004; Powell et al., 2009; Voigt et al., 2008). Furthermore, some taxa of arthropod have reportedly begun practicing geophagy to deal with salt scarcity in plants (Kaspari et al., 2008). Yet despite its pantropical importance~~it has been hitherto~~ , salt availability has hitherto been overlooked in most ~~biogeography and biogeochemistry~~ biogeographic and biogeochemical studies (Dudley et al., 2012). By far, the most important source of continental sea salt depositions are the oceans. ~~In the Amazon, shielded by the natural orographic barrier of the Andes, to the West,~~ Sea salt scarcity in ~~rain water~~ Amazonian rainwater increases along a gradient from the Atlantic coast towards the ~~eastern declivity of the Andes. Both, Na^+ and Cl^- concentration in rain water diminished significantly with~~ Andean range, which acts as a natural orographic barrier to the West. The concentration of both sodium and chloride in rainwater diminishes significantly with increasing distance from the Atlantic Ocean (Talbot et al., 1990). Additionally, the ratio between both concentrations inverts from $Cl^- > Na^+$ close to the ocean to $Cl^- < Na^+$ far from the ocean (Tardy et al., 2005). Consequently, tropical mountain forests on the ~~Andes eastern slopes~~ eastern slopes of the Andes and tropical lowland forest at the western edge of the Amazon are expected to suffer from sea salt deprivation, ~~as opposed to~~ whereas forests closer to the Atlantic coast ~~, where salt deposition is large~~ are subject to large sea salt deposition (Dudley et al., 2012). ~~Particularly in the former, there is evidence that herbivore and frugivore birds and mammals visit mineral licks to compensate for low sodium concentration in plant and fruit tissues in the Amazon of Peru, Ecuador, and Colombia . Some arthropod taxa in the West Amazon have also been reported to practice geophagy to deal with salt scarcity in plants .~~

The tropical mountain forests at the eastern Andean slopes in southern Ecuador may likely represent an exception of this generalized pattern because of their location in the Huancabamba depression, an area where the Andes rarely exceed ~~altitudes >~~3600 m ~~, which might represent a better connection to the Pacific salt sources. In consequence~~in altitude. This allows the transport of Pacific air masses rich in sea salt. As a result, the mountain forest might benefit not only from sea salt transported by easterly air masses from the Atlantic but also by sea salt originating from Pacific air masses. Depending on the strength of the contribution to sodium ~~deposition from~~ and chloride deposition originating from the Pacific, the combined ~~sodium~~ input from Atlantic and Pacific sources could result in a greater ~~salt~~ sodium and chloride availability than that found for the lowland forests ~~in~~ on the western rim of the Amazon (Dudley et al., 2012).

~~However, only few research has been conducted to investigate~~

However, little research has investigated the deposition of atmospheric sodium and chloride in the tropical forests of the ~~South-Ecuadorian Andesand~~ southern Ecuadorian Andes. Furthermore any such research has yet to identify their sources. In this context, an investigation of the deposition by occult precipitation (OP) is particularly important, because OP comprises an extremely high proportion of total precipitation in tropical mountain forests. OP is the water supplied to soil or vegetation by light drizzle, wind-driven rain and fog and/or clouds that conventional rain gauges

cannot measure. An exception is the work of Fabian et al. (2009), who estimated the origin of ~~salt deposited aerosols~~ the local sea salt deposition by visual interpretation of single back-trajectories. To our knowledge, ~~no~~ neither a comprehensive quantitative investigation on sea salt sources nor any ~~estimations~~ estimates of their contribution to the atmospheric deposition have been conducted yet.

As a consequence of the knowledge gaps regarding the sea salt sources of deposition in the Andes of south-eastern Ecuador, the aims of ~~the present study are~~ this study are as follows: (1) to characterize sodium and chloride atmospheric deposition by rain and ~~occult precipitation~~ OP along an altitudinal gradient and at different ~~topographical~~ topographic locations in a tropical mountain rain forest site, (2) to ~~allocate potential geographical sources in the Pacificand Atlantic oceans applying potential source contribution function (PSCF) and concentration weighted trajectory (CWT) analysis~~identify potential Pacific, Atlantic and continental geographic sources of sea salt concentration over the Andes of southern Ecuador by applying back-trajectory statistical techniques and reanalysis data of atmospheric composition, and (3) to estimate the contribution of each source area to the ~~deposition of sodium and chloride in our study area~~atmospheric sea salt concentration in the Andes of southern Ecuador.

2 Study area

The study area is located at the north-western edge of the Amazon basin (4° 00' S, 79° 05' W), at the ~~southeastern~~ south-eastern Andes of Ecuador, approx. 100 km straight line distance away from the Pacific coast and around 2000 km from the closest part of the Atlantic coast ~~. The central study area comprises theRio San Francisco~~ (Fig. 1). The study area contains the*San Francisco* valley, deeply incised into the eastern slope of the main Andes ~~Cordillera~~range. Since 2002, ~~the Reserva Biologica San Francisco~~ two successive multidisciplinary research programs have investigated the *Reserva Biológica San Francisco* (RBSF), located on the northern slopes of the valley and some areas outside of the reserve ~~have been the subject of investigations from two successive multidisciplinary research programs~~ (Beck et al., 2008; Bendix et al., 2013)

The Andes in this area are characterized by lower elevations and ~~a highly~~ higher geomorphological complexity compared to other parts of the mountain chain in northern Ecuador, Peru, and Colombia. ~~Because it is proven~~ Since studies have shown that exposure and altitude ~~affects deposition~~ affect deposition patterns (Griffith et al., 2015; Kirchner et al., 2014; Lovett and Kinsman, 1990; Makowski Giannoni et al., 2013) ~~the current investigation~~ a precondition for the study of sea salt deposition is to collect measurements along a large altitudinal gradient and at different slope exposures~~is the precondition to unveil salt deposition. The valley of San Francisco facilitates such a study design because of its rough terrain~~.

The climate of the catchment is mainly determined by the ~~activity of the constant easterly trade winds~~

from north and south-east, being those from the north-east dominantconstant tropical Easterlies. However, because of the low altitude of the mountains when the trade winds weaken at the end and beginning of each year , are weakened each year between November and March and westerly wind bursts occur , carrying with them locally because of the low altitude of the mountains. Those westerly winds are transporting Pacific air masses into the study area (see Fig. 1)1, Bendix et al., 2008a; Emck, 2007). Precipitation responds to the migration of displacement of the intertropical convergence zone (ITCZ) and the dynamics of the easterly trades. The season of intensity of the tropical Easterlies. The highest rainfall occurs between June and August, when the easterly winds predominate, carrying masses of humid air humid air masses from the lowlands of the Amazon. The topography forces the humid air to move upwards leading to high rainfall sums totals, especially in the higher parts of the mountainsand facilitates the immersion of peaksinto clouds resulting in occult precipitation (OP) , and the peaks' immersion into the clouds, resulting in OP (Bendix et al., 2006, 2008b; Richter et al., 2013; Rollenbeck et al., 2011). The average rainfall varies between In the period 2004 to 2009 average rainfall varied from 1500 and to 6500 mm per year between 1960 and 3180 mfor the period 2004 to 2009. . In the highest parts OP contributes to regions OP contributes up to 35% of total precipitation (Rollenbeck et al., 2011). A short dry season occurs between November and March where when Pacific air masses are transported with occasional westerlies to the area with frequencies by occasional Westerlies. Such air masses occur less than 20% of the time (Richter et al., 2013) and accompanied with thunderstorms and are accompanied by convective activity.

3 Data and methods

The methodology we used is divided into two main parts: The analysis of the concentration of is comprised of two components. First, we analyze local salt (sodium and chloridein rain and OP samples, and the allocation of potential sources of salt by a method that combines air-mass back-trajectories and reanalysis data of sea salt concentration in the atmosphere. Because of the complexity of the terrain, in the first part we assessed the levels of) concentrations by assessing the sodium and chloride concentration concentrations in samples of rain and OP from different meteorological stations (MSs) along an altitudinal gradient, as well as the temporal variation in the concentration at each elevation. To make a first evaluation of the possible origin of sodium and chloride we have also analyzed its relationship to the other ions analyzed using a principal factor analysis. To do so, we use a statistical approach due to the complexity of the terrain. Second, we attempt to derive the source of the salt. The second part focuses on the description of describing the transport pathways associated with the general atmospheric circulation patterns , the detection of potential sources of salt, and their contribution to the transport of salt to our 1000to detect potential source areas of sea salt. Our goal is to draw connections between the contributions each respective atmospheric sea salt

source has on our study area. ~~As done for the concentration data from MSs, the temporal variation of air-mass transport and source contribution was accounted for by assessing its seasonal patterns. The next sections deepen into the materials and methods outlined in this introductory paragraph~~Back trajectory analysis was used to achieve this goal.

3.1 Sample collection~~and~~, materials, and data

Three ~~MSs have been~~ meteorological stations (MSs) were installed on the north-facing slopes of the ~~Rio San Francisco~~ *San Francisco* valley along an altitudinal transect ranging from 1960 to 3180 m in elevation. A fourth station (*El Tiro*, 2725 m) was installed ~~about four kilometers up-valley~~ at a mountain pass about four kilometers up-valley on the Cordillera Real (Fig. ~~1~~1).

~~Regular rain and OP sampling has been carried out at all stations from~~ Rain and OP samples were collected at each station between 2004 ~~to~~ and 2009. While rain water ~~is collected in conventional totalling~~ was collected in totaling gauges (UMS 200; made of ~~Polyethylen~~ polyethylene to warrant chemical inertia), ~~occult precipitation is collected by~~ OP was collected in 1 m^2 mesh grid fog collectors ~~following the design proposed by~~ designed according to Schemenauer and Cereceda's proposal (Schemenauer and Cereceda, 1994). Details about rain and fog measurement techniques, calibration, and data handling are described in Rollenbeck et al. (2007), Fabian et al. (2009), and Rollenbeck et al. (2011).

Rain and OP samples were collected ~~in~~ at almost regular weekly intervals. The samples were filtered and immediately stored in frozen state~~immediately~~, before being sent to the laboratory for ion analyses. All samples were ~~analysed~~ analyzed at the University of ~~Munich'~~Munich1000s Weihenstephan center (TUM-WZW) for major ions (K^+, Na^+, $NH_4{}^+$,Ca^{2+},Mg^{2+}, Cl^-, $SO_4{}^{2-}$, $NO_3{}^-$~~, $PO_4{}^{3-}$). Cation analyses were carried out by~~). Cations were analyzed according to the inductivity-coupled plasma method (Perkin Elmer Optima 3000), while ~~anions were analyzed by~~ ion chromatography (Dionex DX-210) was used for anions. The detection limits are 0.1 and 0.2 $mg.l^{-1}$ for sodium and chloride, respectively.

The sea salt mixing ratio of the Monitoring Atmospheric Composition and Climate (MACC) reanalysis dataset was used as a proxy for the sea salt concentration in the atmosphere, with a horizontal resolution of 0.75° by 0.75° (Inness et al., 2013). In this dataset, the concentration of sea salt generated by wind stress on the ocean surface was determined based on a source function developed by Guelle et al. (2001) and Schulz et al. (2004) accounting for sedimentation as well as wet and dry deposition processes. The sea salt concentration was integrated for three size bins (0.03 to 0.5, 0.5 to 5.0, and 5.0 to 20.0 microns) and calculated for 60 vertical model levels with the upper model limit at 0.1 hPa (Benedetti et al., 2009; Morcrette et al., 2009). To our knowledge, this is the only available global sea salt concentration data that spans the period covered in this study. Furthermore, this reanalysis dataset has performed well when compared to measured satellite and ground-based data (Benedetti et al., 2009).

3.2 Statistical evaluation of sodium and chloride ion concentration in rain and OP

Since sea spray aerosol consists mainly of chloride and sodium (Millero, 2014), we ~~found adequate to use the concentration of Na^+ and Cl^-~~ used the ion concentration of both elements in rain and OP as proxies of ~~sea-salt~~ sea salt atmospheric inputs into the ecosystem. ~~Being~~ Because sodium is a conservative ion in ~~sea-salt aerosol, Na^+ has been~~ sea salt aerosol, it is often used as ~~reference for sea-salt~~ a reference for sea salt concentration in precipitation chemistry and atmospheric chemistry modeling studies (Jaeglé et al., 2011; Keene et al., 1986; Pozzer et al., 2012; Tardy et al., 2005; Vet et al., 2014). Chloride is more unstable as it photochemically reacts with other atmospheric ions (e.g. sulfur and nitrogen species) and it is depleted as a function of time spent in the atmosphere (Keene et al., 1986).

~~Weekly Na^+ and Cl^- concentration~~

Weekly sodium and chloride concentrations in water samples from rain and OP ~~was~~ were weighted with the total weekly precipitation volume ~~, averaged to monthly means of volume weighted concentration~~ to calculate volume weighted monthly mean concentrations (VWMM). With the calculated VWMM we compiled monthly time-series of sea salt concentration for a ~~6~~ six year time series from ~~2006 to 2009. Additionally~~2004 to 2009, which represented the temporal variation in the concentration at each altitudinal level of the study area. To identify differences in the distribution of sodium and chloride concentrations between the sites we created box plots of total concentration over the six-year evaluated period at each altitudinal level. Additionally, we computed total volume weighted means (VWM) to compare our observations with those from other studies.~~To check for differences in salt concentration between the sites located at different altitudes we computed box plots of total concentration at each altitudinal level.~~

~~Finally, factor analysis was applied to all measured ion species to look for~~

We analyzed the relationship to other ions (K^+, $^+$,Ca^{2+},Mg^{2+}, $SO_4{}^{2-}$, $NO_3{}^-$) using a principal factor analysis (PFA) to locate common transport histories . Before factor analysis was conducted and the likely origin of sodium and chloride. Before conducting the PFA , the data was normalized and scaled to gain achieve comparable distributions.

For sea-salt concentration in the atmosphere we used the sea-salt mixing ratio of

In coastal continental areas the Na^+/Cl^- molar ratio is typically that of sea salt (Keene et al., 1986). This ratio was calculated using the measurements from each altitude and serves as an indicator of the Monitoring Atmospheric Composition and Climate (MACC) reanalysis data set as proxy. The concentration of sea-salt generated by wind stress on the ocean surface are diagnosed based on a source function by and accounting for sedimentation, and wet and dry deposition processes. In this function wet sea-salt mass fluxes at 80 relative humidity are integrated for the three size bins (0.03 to 0.5, 0.5 origin of both sodium and chloride concentration in precipitation. The ratio changes as a function of distance from the ocean, as chloride is photochemically depleted in the atmosphere.

Finally, to 5.0, and 5.0 to 20.0 microns) and sea-salt concentration is calculated for 60 model levels with the model top at 0.1 hPa . asses a likely impact of anabatic flows on the sodium and chloride budget, we calculated wind direction relative frequency plots.

3.3 Back-trajectory Back trajectory and source-receptor analysis

Ten days long back-trajectories The HYSPLIT model was used to generate back trajectories of air masses were generated with the HYSPLIT model encompassing ten days with a resolution of one day (Draxler and Hess, 1998). Modeling was done using the openair R package (Carslaw and Ropkins, 2012) for R statistical language . The wind fields are represented by NCEP/NCAR reanalysis were derived from the ERA-Interim reanalysis (Dee et al., 2011) with a grid resolution of 2.5 0.75 ° by 2.5 0.75 °. All trajectories had their origins at the ground measurement sites from *El Tiro* *San Francisco* and *Cerro del Consuelo* in South-Ecuador river catchment in southern Ecuador . The MACC sea-salt concentration data set reanalysis sea salt concentration data was set as proxy of sea-salt sea salt concentration in the atmosphere for air-mass transport analysis by back-trajectory modeling. Cluster analysis was applied to the back-trajectories to group similar air mass histories and to post process concentration data in relation to cluster origin. Euclidean distance was used as measure of similarity between different trajectories. In a next step we calculated back trajectory techniques. To test the link between the MACC sea salt concentration and the sodium and chloride concentrations actually measured in rain and OP, both were linearly correlated. Pearson's product-moment correlation coefficients were calculated between the concentration at the two uppermost MSs (*El Tiro* and *Cerro del Consuelo*) and the MACC sea salt concentration (see Table1). Based on the correlation coefficients, the frequency of trajectories represented by each cluster to analyze the sea-salt concentration in relation to each of them. Furthermore, we compared the contribution of each cluster to the concentration in the monthly MACC reanalysis sea-salt concentration time-series. The choice of monthly time-series is justified because it permits the post-comparison with the Na^+ and Cl^- measured concentrations MACC dataset at 700 hPa and the medium particle size (0.5-5.0 μm) was chosen as the input parameter for further examination by back trajectory analysis, because it yielded the highest correlation coefficient and significance level .

Given the spatial resolution of the dataset (0.75° by 0.75°), the outcome of this analysis can only provide evidence of synoptic transport pathways and source-receptor relationships for medium to long-distance sources for an area of approximately 80 by 80 km^2 in the southern Ecuadorian Andes. Local-scale transport is not represented by the used trajectory models.

As stated in the objectives, our main goal is We first aimed to identify the potential geographical origin of high sea-salt concentration at the geographic origin of the sea salt concentration over this wider area covering our receptor site in the RBSF southern Ecuador . For this particular purpose we

used source-receptor modeling as it has been successfully applied to determine likely geographical geographic origins of pollutants and aerosols (e.g., Fleming et al., 2012; Hsu et al., 2003; Powell et al., 2009; Riuttanen et al., 2013; Robinson et al., 2011). Here, two different hybrid receptor models for comparison were used : the PSCF were used for comparison: the potential source contribution function (PSCF) and the adjusted CWT concentration weighted trajectory (CWT) running on a grid that covers the domain of the 2192 generated trajectories between 2004 and 2009. Given the high seasonality of synoptic air mass transport, we calculated the models on a seasonal basis (Bendix et al., 2008a; Emck, 2007).

The PSCF (Malm et al., 1986; Pekney et al., 2006; Zeng and Hopke, 1989) calculates the probability that a source of aerosol or pollutant observed at the ground measurement site is located at a specific cell in the geographical geographic space and is defined by:

$$PSCF_{ij} = \frac{m_{ij}}{n_{ij}} \tag{1}$$

where n_{ij} is the number of trajectory points that passed through cell (i,j) and m_{ij} is the number of times that trajectory points passing through the cell (i,j)correspond to high concentration values , correspond to a high seas salt concentration (above an arbitrary threshold) at the time of arrival of the trajectory to the trajectory's arrival at the receptor site. The function is based on the premise that, if a source is located at that specific location, the air masses represented by the trajectory passing through the collocated cell are likely to collect and transport the material along the trajectory until the receptor site. In this study, we defined two concentration thresholds: the 75th 75^th percentile for moderate-to-high concentration and the 90th percentile for only 90^th percentile for high concentration.

The adjusted CWT function uses a grid domain to calculate a grid-wise logarithmic mean concentration of an aerosol or pollutant (Seibert et al., 1994) and is defined by:

$$ln\left(\overline{C}_{ij}\right) = \frac{1}{\sum_{k=1}^{N} t_{ij}} \sum_{k=1}^{N} ln\left(\overline{C}_k\right) t_{ijk} \tag{2}$$

where i and j are the grid indices, k the trajectory index, N the total number of trajectories, $\overline{C}_k$ the pollutant concentration measured upon arrival of trajectory k, and t_{ijk} the residence time of trajectory k in grid cell (i, j). In this method, a weighted concentration is assigned to each pixel in the domain. This concentration is the average of the sample concentration at concentrations at a given receptor that have associated trajectories crossing the respective cell.

In a second step, we assessed the contribution of the main transport pathways of sea salt to the observed concentration over southern Ecuador. For this purpose we integrated the MACC sea salt

data to the back trajectory cluster analysis. As for the source-receptor modeling approach, cluster analysis was applied on a seasonal basis to group similar air mass histories. This revealed general circulation patterns and, subsequently, post-process concentration data in relation to cluster origin and pathways. A partitioning algorithm based on spherical k-means was used to define the appropriate number of trajectory clusters, as well as prior knowledge of the main wind systems affecting the receptor site. We tested different k-values and chose the maximum number of cluster objects (i.e. back trajectories) that most closely reproduced the known conditions. The cosine distance was used as measure of similarity/dissimilarity between different trajectories. Afterwards, the frequency of trajectories represented by each cluster was determined.

To estimate the contribution of the different seasonal transport pathways to the observed sea salt concentration, the single trajectories belonging to each cluster object (cluster mean trajectory) were related to the sea salt concentration in the nearest neighboring pixel within the study area. In this way, the contribution of each cluster object to the sea salt concentration above the study site could be statistically evaluated. Likewise, to analyze sources and sinks of sea salt along the cluster mean trajectories, we extracted the mean seasonal concentration values from the MACC data pixels (from 2004 to 2009) that matched the cluster mean trajectories in location, time, and height. Seasonal sea salt concentrations maps were calculated to further interpret the concentration along the cluster mean trajectories. For this, the MACC sea salt data was vertically integrated between 875 hPa (the minimum height of the trajectory clusters) and 500 hPa (maximum height). Additionally, based on findings by Akagi et al. (2011) showing that burning biomass is a contributor to chloride emissions, the Copernicus atmosphere monitoring system's (CAMS) global fire assimilation system (GFAS) (Kaiser et al., 2012) was used to create seasonal maps of NO_x biomass burning fluxes over South America.

4 Results

4.1 Sodium and chloride concentration

Since our Our study area is characterized by the intricated complex topography of the Andes (see Fig. 1), we first examined the 1). Hence, temporal variation and distribution of the is of interest in our study of sodium and chloride concentrations in rain and OP from MSs at different altitudes and topographical locations.

Figure 2 (left column) depicts the time-series of Na^+ and Cl^- concentration from MSs time series of sodium and chloride concentrations at different altitudes. *Cerro del Consuelo* meteorological station (MS) MS , situated at 3180 maltitude, presents , demonstrated the clearest temporal pattern in the concentrationof salts concentration , where the highest peaks take place occurred

almost regularly between September and February (Fig. 2a).For Na^+ the highest peaks are found in the MSs of The highest concentrations of sodium were recorded at *Cerro del Consuelo* and *El Tiro* (2825 m) and *Cerro del Consuelo* (Fig. 2 a and d). Opposed to this, Cl^- b). Contrarily, chloride concentration peaks in OP are were highest at the lowermost lowest MS, ECSF (Fig. 2, c d).

To compare the respective distributions, the boxplots in Fig. 2 (right column) show the concentration of sodium and chloride for both , rain and OP for each considered at every MS. Overall, no essential variations between the concentration at each MS can could be observed except for Cl^- in OP water at ECSF MS chloride in OP and rainwater at ECSF (Fig. 2 d), that presented values where reported values were much higher than those measured at other elevations. Regarding ion concentration in sodium and chloride species a clear difference can could be observed with Cl^- chloride concentration in the interquartile range extending between 0.22 and 0.51 mg· l^{-1}, and Na^+ sodium concentration extending between 0.06 and 0.20 mg· l^{-1}.

In the rain samples, Cl^- concentration is

In rainwater samples, the concentrations of chloride were considerably higher than the Na^+ concentration at all MSs those of sodium at each MS . A larger spread range and higher extreme values are observed in Cl^- concentration. Na^+ concentration do not present a relevant difference were observed in the chloride concentration. Differences in sodium concentrations between MSs at different altitudes . The concentration show a little were negligible. The concentrations showed a slight increase at TS1 MS (median of 0.14 mg· l^{-1}) and *El Tiro* (median of 0.13 mg· l^{-1}) and decreases decreased again at the highest station, *Cerro del Consuelo* (median of 0.07 mg· l^{-1}). Compared to the rain samples, OP contains contained a higher mean Na^+ and Cl^- concentration concentration of sodium and chloride but also a larger spread greater range in its distribution (Fig. 2, left column). The concentration of Cl^- is also significantly chloride was also considerably higher than that of Na^+, with sodium, with the highest mean concentration (median of 0.62 mg· l^{-1}) at the lowest MSof ECSF. The concentration of Na^+ peaks at *El Tiro* MS , ECSF. Sodium concentration peaked at *El Tiro* (0.17 mg· l^{-1}). At TS1MS , the mean concentration is was lowest (median of Na^+ 0.09 mgl^{-1} for Na^+ and ·l^{-1} and Cl^- 0.3 mgl^{-1} for Cl^-) , increasing ·l^{-1}) increased once again at the highest elevations, *El Tiro* and *Cerro del Consuelo* (median El Tiro and Cerro del Consuelo (median Na^+ between 0.11 and 0.17 mgl^{-1} for Na^+ and ·l^{-1} and Cl^- between 0.33 and 0.35 mgl^{-1} for Cl^- ·l^{-1}).

To gain some insights on

A PFA of every major ion concentration was conducted to gain insights into the origin of salt inputs, a factor analysis of all analyzed major ion concentration from the MSs was conducted. The analysis indicates four components which explain most sea salt inputs for each MS (Table2). This analysis indicated four components that explain the majority of the variability in the dataset. Na^+ and Cl^- have large loadings on factors The load of sodium and chloride had a considerable bearing

on either factor 1 or 2, depending on the MS's altitude and location of the MS , and the precipitation type. This two factors explain These two factors explained at least 29% of the variability in the system (Fig.3 Table2).

With the exception of the lowermost station (ECSF, 1960 m), Na^+ and Cl^- explain

385 Sodium and chloride explained the greatest variability in the system, in the rain samples. The ECSF station, as shown in Fig.2, presents a different distribution in the chloride concentration than that from MSs at higher elevations system's rain samples, except for TS1 (2660 m) .

At *Cerro del Consuelo*MS, compounds from biomass burning co-dominate , sodium, chloride,

390 and potassium dominated the variability in rain, given that SO_4^-, NO_3^-, Na^+, and Cl^- load to factor 1 (Fig.3a). This means that Na^+ and Cl^- share a common air mass history with NO_3^- and SO_4^- and thus, the salt concentration has most likely an Atlantic origin. they loaded to factor 1. In OP samples, the biomass-burning compounds have such as nitrate, sulfate, and ammonium had a stronger signal, loading to factor 1. Factor 2 represents sea-salt sources only, since solely Na^+ and

395 Cl^- load to factor 2. The origin is most probably the sporadic intrusion from was loaded by sodium and chloride only. No other compounds loaded to this factor, meaning that sodium and chloride most likely originated in sea salt from Atlantic and Pacific air masses.At *El Tiro* MS,

At *El Tiro*, sea salt sources were exclusively present in factor 1 in for rain and factor 2 in OPrepresent sea-salt sources only (Fig.3b). Sea-salt represents the most important factor in rain and the

400 second most important in OP, behind biomass burning sources from the Amazon. for OP, similar to *Cerro del Consuelo*. As for *Cerro del Consuelo*, sea salt explained most of the variance in rain, followed by biomass-burning compounds. The opposite was true for OP, where biomass-burning compounds dominated, followed by sea salt.

405 The situation at TS1 is not so clear compared to was more complex than at *Cerro del Consuelo* and *El Tiro*MSs , given the combined influence of the local valley-mountain wind mountain-valley breeze system and the synoptic system. In rain, Na^+ and Cl^- are dominating biomass-burning compounds dominated the variability, as they present high with significant loadings on factor 1 (Fig.3c) 1. Factor 2 was only loaded with sodium and chloride . In OP, they continue to show high

410 loadings on factor 1 , but this time they share a transport history with NO_3^- and SO_4^- represented sea salt and crustal material, as sodium, chloride, calcium, and magnesium loaded to this factor . In the OP rain samples at ECSFMS, Na^+ and Cl^- load , sodium and chloride loaded to factor 1 together with Ca^+ and Mg K $^+$(Fig.3d) . In the rain samples Ca^+ and Mg OP samples nitrate, SO_4^-, and K $^+$ dominate dominated the variability loading to factor 1, while Na^+ and K^+ load

415 sodium and chloride loaded to factor 2.Cl^- does not play any role in this type of precipitation.

4.2 General transport pathways and spatial allocation of sources

In the last section we analysed the temporal and altitudinal concentration of Figure 3a shows the $Na^+$and / Cl^- concentrations in the deposition through rain and OP , and related them to the other ions measured in deposited rain and OP water . The remaining question of where the Na^+ and Cl^- source areas are located geographically is elaborated in this subsection. To spatially locate the sources we used HYSPLIT back-trajectories and MACC sea-salt concentration. Based on a correlation analysis between molar ratio calculated in data from OP and rain water samples collected at each MS along the altitudinal gradient studied. The typical molar $Na^+$and / Cl^- concentrations in rain and OP measured at the two uppermost MSs (*El Tiro* and *Cerro del Consuelo*) and the reanalysis sea-salt concentrations for three size bins at six common pressure levels (see Table**??**) three different target altitudes were selected: 3180 m which is the altitude of the highest MS *Cerro del Consuelo* and already infringes the lower tropospheric layer, as well as two other target altitudes that penetrate deeper into the synoptic layer (4200 and 6000 m). We chose the MACC dataset at 700 hPa pressure level and the medium particle size (ratio in precipitation for areas close to the sea is 0.86 (dotted line in the figure), according to Keene et al. (1986). The International Co-operative Programme on Assessment and Monitoring of Air Pollution Effects on Forests (ICP) recommends an acceptable range of values between 0.5 -5.0 micrometers)as input parameter for the backward trajectory analysis because it yielded the highest correlation coefficient and significance level. That being so, it demonstrated to best represent the conditions observed at the ground measurement site.

Trajectory cluster analysis was applied to identify the main representative air mass transport patterns, and so the transport pathways of sea-salt (Fig.4, Fig.5 and Fig.6). As shown in panel (a) of Fig.4 - Fig.6 the easterly winds are dominant at all tested target altitudes. For the lower height levels (panel a and 1.5 molar units (Clarke et al., 2010) (dashed line in Fig. 5 and Fig.6)the clustering results were very similar, where predominantly fast flowing east trajectories characterize the air mass transport (from approximately 87 to 90 of the trajectories), and less frequent slower moving trajectories from the west (between approximately 9 and 10) appear rather sporadically. At 6000 meter height level the air flow speed increases in both, easterly (approximately 92) and westerly (approximately 8) trajectories (Fig. 4a).The latter lose its vortex-like sweep as in Fig.5a and Fig.6a, as a result of a decreasing influenceof the transport of air masses along the Peruvian coast. In Fig.4a, only cluster six (C6) originates in the Equatorial Pacific, while cluster four (C4) moves to the north. Cluster three (C3) originates east of the RBSF, flows across the Andes and over the Pacific and turns back towards the east to finally reach the receptor site. This type of bow-shaped trajectories is common to all three target altitudes (Fig.4a, C3; Fig. 5a, C4 and C6; and Fig. 6a, C3, C4, and C5) and characterizes the coastal wind system associated with the Humboldt current . 3). Outliers were likely due to samples with concentrations too close to the detection limits. When approaching the lower limits of the concentration, the ratio becomes more unstable and tends towards more extreme

values.

The mean sea-salt concentration for the trajectory clusters arriving at the RBSF is presented in Table2. The Pacific clusters (Table2 C3, C4

The highest stations show a stronger marine influence , C5 for 3180 m, C4, C5, C6 for 4200 m, and C3, C4, C6 for 6000 m) reveal a higher concentration of sea-salt, whereas easterly air passing over the Atlantic and the South American continent before arriving at the RBSF show intermediate to lower concentrations. North-easterly trajectories for example were associated with an intermediate concentration, while easterlies and south-easterlies had only small concentrations related to them. In addition to the cluster-associated mean NaCl sea-salt concentration it is also valuable to know in which proportion each cluster adds to particularly in OP. The ratio fluctuates within the acceptable range and is mostly close to the total concentration in the analyzed study period. The values in parenthesis in Table2 summarize the contribution in percentage of each cluster. For the trajectories arriving at 3180 and 4200 m height level (Table2) cluster C1, representing the north-easterlies, had the highest contributions. Furthermore, once added the contribution from the other two easterly clusters (Table2 C2 and C6 for 3180 m, C2 and C3 for 4200 m, and C2 and C5 for 6000 m), approximately 74 to 80 of the total concentration is associated with an easterly transport of air masses coming from the Atlantic. The remaining 20 to 25 are attributed to air flows passing over the Pacific before reaching the RBSF. These highly loaded seasonal Pacific flow incursions take place in the southern hemisphere's late-spring and summer as easterlies weaken due to the south-ward shift of the ITCZ. This pattern is clearly shown in panel b) of Fig.4 - Fig. 6, where sea-salt time-series describe the proportion of concentration contributed by each cluster. Atlantic air masses add to the concentration constantly along the year, also in winter, when the Pacific flows does not play any role. However, the high peaks at the end and the beginning of each year are clearly dominated by standard value of sea salt in precipitation from coastal areas. This influence diminishes as the altitude decreases, especially for OP. Median ratios of 0.7, 0.8, 0.5, and 0.3 for *Cerro del Consuelo*, *El Tiro*, TS1, and ECSF, respectively, also reflect a greater influence of sea salt at higher altitudes.

A somewhat stronger seasonal behavior was identified at the two highest stations (gray columns show the transport from the Pacific.The same seasonal patterns were also identified in the measurements in Fig. 2, being clearest at the highest station period from September to February, with the highest frequency of intrusion by the Easterlies). Figure 3b depicts the frequency of trajectories on a yearly basis. In the first three years (2004-2006) the occurrence of Westerlies was more frequent and at the same time the Na^+/Cl^- ratio was close to that of fresh sea water (local Pacific influence). During 2007-2009, when Easterlies were more frequent, the Na^+/Cl^- ratio increased due to the increasing influence of distant Atlantic sources (chloride is depleted during transport) and the likely

contribution of forest and agricultural fires (Reid et al., 2004; Akagi et al., 2011).

Locally driven winds, such as thermally-induced anabatic winds, can contribute to the transport of local sodium and chloride from the valley to the upper parts of the catchment. In a previous study, however, Makowski Giannoni et al. (2013) showed that anabatic winds do not impact MSs located on mountain tops, where synoptic winds predominate. Figure 4a and b show relative frequencies of the wind direction at ECSF and *Cerro del Consuelo*, respectively. At the lower altitudes (ECSF) a typical mountain-valley breeze circulation system exists, while at the crest (*Cerro del Consuelo*(Fig.2a), which means that it is possible to explain the observed patterns in the measurements by) northeasterly wind directions predominated.

4.2 Spatial allocation of sources and general transport pathways

In the previous section we analyzed the temporal and altitudinal variation of sodium and chloride concentrations in deposition driven by rain and OP. This section addresses the remaining question of where the sodium and chloride source areas are located geographically.

The synoptic wind system over South America is driven by strong seasonal circulation patterns. Because the air mass transport to the receptor site is directly linked to the seasonal cycle of the large-scale atmospheric circulation patterns. circulation system (Bendix et al., 2008a; Emck, 2007) and thus, sources of sea salt concentration and their intensity may vary with the seasons, we examined seasonal patterns present in the sources and dominant air mass trajectory clusters.

After characterizing the main pathways of air masses on the basis of back-trajectories and cluster analysis, we take a look at potential sources which might contribute to the sea-salt We first evaluated potential contributory sources to sea salt concentration at the receptor site for each season . For this reason purpose, the two hybrid receptor models were used as shown in Fig. 7. In order to capture source areas responsible of moderate and high concentration contributions at the receptor site we applied the PSCF with two distinct predefined concentration thresholds, the 75th and the 90th percentiles, 5. In accordance with a sensitivity analysis done with back trajectories starting at different altitudes, these functions were applied to 3180 m, the altitude of the MS *Cerro del Consuelo*, on top of the highest peak in the catchment. Trajectories starting at lower altitudes have greater uncertainty because local flows are driven by the complex topography and cannot be reproduced. Those starting at higher altitudes provided no further information as they have coincidental source areas.

Figure 5 shows the spatial distribution of potential sources calculated by the PSCF (a, b) and the CWT function, which inherently discriminates between sources of moderate and high intensity. In

accordance with the back-trajectories these functions were applied for three selected height levels of 6000, 4200, and (c), for DJF, MAM, JJA, and SON at 3180 m (Fig.7).

starting height at the receptor. When we compare the spatial distribution of potential sea-salt sources between the two models (PSCF and CWT), similar locations in the Atlantic and Pacific Oceans can be observed are indicated . The highest probabilities/concentration (above 0.5 likelihood (concentrations above $5e^{-9}$ for Fig. 7a-f 5a and b and above $5e^{-9}$ for Fig. 7g-h) occur in the equatorial Pacific 5c) is an equatorial Pacific location , which points to stronger sources of sea-salt sea salt in that region contributing to the high concentration at the receptor siteand confirms the results of the trajectory cluster analysis in Table2. The target altitudes of the back-trajectories (left, middle and right columns in Fig.7) show a generally coinciding location of source transport pathways. However, at the lowest target altitude (Fig.7, right column) the transport along the coast of Peru becomes more important due to the increasing influence of the lower tropospheric wind system .

High sea-salt emission sources are expected to be found whether in Strong sources of sea salt are expected from either the Pacific or in the Atlantic. To judge from the high probabilities/concentration over probability that the concentration stems from the oceans, the PSCF with 90th percentile threshold (Fig. 7d, e, f results of the PSCF (90^th percentile concentration threshold, Fig. 5b) and the CWT (Fig. 7g, h, i 5c) performed best in discriminating between potential geographical sources that contribute geographic sources that contributed to moderate and high sea-salt concentration at RBSF in South sea salt concentrations over southern Ecuador. In contrast, the PSCF with 75th percentile when using the 75^th percentile as the concentration threshold (Fig. 7a,b,c) 5a) the PSCF only detected the transport pathways for sea-salt sea salt irrespective of the intensity of the source contribution to the concentration.

4.3 Seasonal patterns in sea-salt transport and source contribution

The synoptic wind system over South America is driven by strong seasonal circulation patterns. Because the air mass transport until Seasonal source contributions that had the greatest impact, i.e. responsible for high sea salt concentrations at the receptor siteis directly linked to the seasonal cycle of the large-scale circulation system and thus, sources of sea-salt concentration and their intensity may vary with seasons we examined if seasonal patterns are present in the dominant clusters for each height level. For this reason the sea-salt concentrations related to each clusters were separated by months and years to get an overview on its temporal variations. , occurred between September and February (September, October and November [SON] and December, January and February [DJF]). During SON, the equatorial Pacific was the dominant source, while in DJF both the Pacific and Atlantic sources contributed to the concentration. Yet, the Pacific sources still appeared stronger, as indicated by the large number of high values in that area. Furthermore, chlorine-containing com-

pounds related to sea salt and biomass-burning were likely co-linearly transported during that season, as shown by the high concentration over the northern portion of South America during DJF, and the coincidence of the biomass-burning season in that area (Fig. 9). On the other hand, during austral autumn (MAM) and winter (JJA) the models identified no relevant potential sources of high sea salt concentration.

Figure 8 illustrates the mean sea-salt concentration for each cluster and the three distinct height levels analyzed. Based on the highest values in austral late spring (SON) and summer (DJF) , when mean concentration are frequently above 8e-9 kg kg^{-1}, it is evident that the highest mean sea-salt concentrationis related to the westerly and north-easterly air masses.During this time the western and north-eastern clusters also present a more or less strong seasonality (clusters C3, C4, C5 and C6 in Fig. 8a; clusters C1, C4, C5 After locating the potential geographic sources of sea salt, trajectory cluster analysis was applied to identify the main representative air mass transport patterns, and C6 in Fig. 8b, thus the transport pathways of sea salt (Fig. 6). Here, the Easterlies were dominant. In the air mass transport, fast flowing east trajectories dominated (from approximately 83 % to 97 % of the trajectories, in DJF and JJA, respectively), and clusters C1, C3, C4 and C5 in Fig. 8c) owing to the fact that westerlies are only present slower-moving trajectories from the west appeared rather sporadically (between approximately 2.8 % and 17 %). The occurrence of bow-shaped trajectories was common (Fig. 6, MAM and DJF) and characterized the coastal wind system associated with the Humboldt current (Bendix et al., 2008a; Emck, 2007).

Westerlies mostly evolved during SON and DJF, while north-easterlies are and to a lesser extent during MAM. Meanwhile, North-Easterlies were absent during the austral winter (JJA) following the migration displacement of the ITCZ to the north. The eastern and south-eastern clusters exhibit clusters exhibited no seasonal pattern, because they are represent the prevailing wind directions throughout the year.The sea-salt concentration associated with these clusters is much weaker, but

Table3 summarizes the mean sea salt concentration over southern Ecuador related to each cluster object reaching the receptor site for each season. High concentrations of sea salt are associated with westerly and north-easterly trajectories mainly occurring between September and May (Table3), whereas easterly air masses that passed over the Atlantic and continental South America before arriving at the receptor site showed intermediate to lower concentrations. In addition to the cluster-associated mean sea salt concentration, values in parenthesis in Table3 describe the proportion (in percentage) that each cluster contributes to the total concentration during the study period. Cluster C2, representing the North-Easterlies, was associated with the highest contributions in DJF and MAM. In SON, cluster C2 represented the Easterlies and was likewise associated with the highest contributions. SON is the main biomass-burning season in the Brazilian Amazon, which likely contributed to the overall budget. Furthermore, Easterlies transport from September to May was as-

sociated with approximately 75 % to 80 % of the total concentration. The remaining 15 % to 20 % were attributed to air flows passing over the Pacific before reaching the receptor site. These highly loaded seasonal Pacific flows took place in the southern hemisphere's late-spring and summer as Easterlies weaken due to the southward shift of the ITCZ. Atlantic air masses contributed to the concentration constantly over the year, also in austral winter (JJA), when the Pacific flows were negligible. However, transport from the Pacific clearly dominated the high peaks at the end and the beginning of each year. The sea salt concentrations associated with the easterly clusters was much weaker. However, due to its high frequencyit contributes more continuously , it persistently contributed to the transport of background concentration from the Atlantic . with likely additions from Amazon fires. Similar seasonal patterns were also identified in the measurements as illustrated in Fig. 2, the most clearest of which occurred at the highest station *Cerro del Consuelo* (Fig. 2a). That means that the observed patterns in the measurements can be explained by the large-scale atmospheric circulation patterns.

Again, to look for seasonality in the location of potential sources we calculated seasonal PSCF and CWT maps. Figure 9 and Fig. **??** show the spatial distribution of potential sources for the PSCF (90th percentile)and the CWT for DJF, MAM, JJA, and SON at the 3180 m receptor height level only. The two remaining height levels at receptor site are not shown because they give no further information. The sources that have the greatest impact, i.e. responsible for Figure 7 depicts the sea salt concentration along the cluster mean trajectories and the trajectory height for each season. The north equatorial Atlantic was a great source of sea salt during DJF (Fig. 7, column 1), according to the sea salt concentration along the trajectory clusters. Nonetheless, the high sea-salt concentrations at receptor site , occur between September and February (DJF and SON). During SON the source on the equatorial Pacific is dominant, while in DJF both Pacific and Atlantic sources contribute to the concentration. Yet, the Pacific sources still appear stronger, as indicated by the high concentration of pixel with high probability values in that area. On the other hand, during austral autumn (MAM) concentration rapidly decreased as the air masses traveled over the continent. Compared to westerly air masses, easterly air masses were lower in elevation, which increased the probability that they were loaded with aerosols from surface emissions. Those air masses then ascended abruptly as they approached the Andean range. In comparison, the equatorial Pacific is a less significant source for sea salt. Because of its vicinity to the receptor site and winter (JJA) no relevant potential sources of high sea-salt concentration were identified by the models. because the air masses spent most of the time over the ocean, the concentration did not sink significantly over time (Fig. 7, C4-C6). The concentration peaks in C1 and C2 were due to sea salt intrusions from the Caribbean Sea and canalized by the Andean cordillera, as depicted in Fig. 8. The season DJF was also characterized by frequent forest and agricultural fires in northern South America, which likely contributed chlorinated

compounds from biomass burning to the budget as well (Fig. 9).

A similar situation also occurred in MAM (Fig. 7, column 2), where C1-C3 are north-easterly air masses and C4-C6 represent westerly pathways. In C2 the intrusion of sea salt from the Caribbean was also present, but less pronounced than in DJF (Fig. 8).

For SON (Fig. 7, column 3) most of the budget was transported from the Atlantic and the continent: clusters C1, C2, and C3. Because this period coincided with the Brazilian biomass-burning season (see Fig. 9), a considerable quantity of sodium and chloride from the Atlantic (Fig. 8) and from fire emissions were probably transported to the receptor site.

5 Discussion

In this study we examined potential sources of Na^+ and Cl^- observed in rain and OP along an altitudinal gradient in the south-eastern sodium and chloride for the southern escarpment of the Ecuadorian Andes. The analyses were carried out by back-trajectory investigation analyzed chemical ion concentrations in rain and OP samples along an altitudinal gradient, using back trajectory statistical analysis and two source-receptor models modeling .

Owing to the rough terrain, we

We first explored the distribution of sodium and chloride inputs by rain and OP measured in the study area in dependence of the altitudeand thus, its wind exposure in relation to altitude . Overall, comparisons between the MSs revealed reveal a difference in the temporal variation of the concentration of Na^+ and Cl^- sodium and chloride in rain and OP depending on the elevation and exposure. Moreover, the highest MS The highest MS, *Cerro del Consuelo*described , displays a distinct seasonal pattern, which is otherwise lacking or less accentuated for pronounced at the remaining MSs. The largest concentration in deposited water of water deposition occurred between September and February, concomitantly with the southward migration of the ITCZ and the more frequently occurring north-easterly winds frequent North-Easterlies (see Fig. 2). Regarding the total concentration , Cl^- was always considerably higher than Na^+

Chloride was consistently a larger portion of the concentration than sodium , which agrees with findings by Tardy et al. (2005). In their study , they Their study investigated the chemical composition of rain water rainwater in the Amazon and found Cl^- concentrations being higher than Na^+ in places close that in places closer to the Atlantic ocean, while the places located Ocean chloride concentrations were higher than sodium, whereas this ratio inverted for locations further away from the Atlantic coastpresented a higher Na^+ than Cl^- concentration . The observed excess in Cl^- concentration chloride concentration compared to sodium at our study site compared to

Na^+ means that there is a relevant influence from the Pacific ocean, indeed, despite the barrier effect of the Andes for the transport of air masses. means that marine sources have a significant impact on the overall sea salt presence. This influence is also demonstrated by the Na^+/Cl^- molar ratios in samples from the MSs along the altitudinal gradient. Higher altitudes are exposed to synoptic circulation and stations there register Na^+/Cl^- ratios closer to that in marine air masses. This indicates a gradient of sea salt inputs with relation to terrain height.

Through factor analysis it was possible to describe how sodium and chloride are related to the other elements measured and thus, to identify if common pathways are present that could give us hints on the possible origin of sodium and chloride. To conclude from contributions to

Common transport histories were identified on the basis of the PFA. As evinced by their prevalence in the first two components, sea-salt represented by sodium and chloride had a strong relevance in both , concentration are very relevant in both rain and OP. Two likely origins could be approximated depending on the location of sodium and chloride in the multidimensional space: east (presumably the Atlantic), when the The fact that they exclusively load to factor 1 or 2, based on their location in multidimensional space, suggests the likely origin of sodium and chloride air mass history was shared with elements of Amazon biomass-burning emissions (nitrate and sulfate, as revealed by) and west (probably the Pacific Ocean), when sodium and chloride presented an individual and unique air mass history. The latter means that solely is sea salt from either the Pacific or the Atlantic Ocean. Biomass-burning seems to play a minor role in the transport of sodium and chlorideload to a factoras depicted in Fig. 3. Considerng that, at *Cerro del Consuelo* MS rain was more associated with an Atlantic origin of sodium and chloride , and OP with a Pacific origin (Fig.3a) . At *El Tiro* MS it is the other way around, with sea-salt from rain having more a westward origin and that from OP more a eastward origin (Fig.3b) . Source partitioning by factor analysis also allowed to identify the effects of local winds and pollution in the , since nitrate and sulfate did not load to the same factor. Although emissions of chloride from fires may be recognizable (Akagi et al., 2011), they are likely irrelevant compared to sea salt (Fabian et al., 2009). Calcium and magnesium (crustal material) loading to factor 2 in OP at TS1 (Table 2) reveals the effect local winds have on emissions at lower elevations. The influence of chloride-containing dust blown from the Loja-Zamora road and biomass-burning (Fig. 1) and plumes from local biomass-burning fires are the most likely cause causes of the high chloride concentration at the ECSFMS concentrations at ECSF . Findings by Yokouchi et al. (2002), Spanos (2002), Hildemann et al. (1991), Akagi et al. (2011), and Harrison and Pio (1983) substantiates substantiate this assumption. According to these studieschloride does , chloride not only stems from sea-spray sea spray but is also emitted from natural and anthropogenic terrestrial sources, namely dust, biomass-burnig i.e. dust, biomass-burning and biogenic forest emissions.This can be inferred from the time-series and factor analysis

Concluding from the ion concentration time series (Fig. 2and 3)too. The) and PFA (Table 2), the distribution of chloride and its relation to other ions are distinct between valley and the mountain tops, where the concentration in the former sources can differ between valleys and mountain tops. In the former, the concentration is influenced by local winds and emissions, while that in the latter depends most likely only from the the concentration most likely depends on synoptic air-mass transport and emissions from distant sources. Being a conservative ion, sodium has very few sources others than ocean spray. This property of sodium is reflected in the time series (Fig. 2), in that no influence of local sources could be noticed This difference in atmospheric circulation between valleys and mountain tops is clearly depicted in Fig. 4, in which only the mountain tops are strongly influenced by the synoptic circulation .

To determine the relevance of Pacific sources to the sea-salt transport into the study area, back-trajectories statistical analysis and

The potential sources defined by PSCF and CWT were used. Three different height levels were considered for analyzing the pathways of air mass transport (see Fig. 4 - 7) . On the basis of a cluster analysis, the trajectories could be grouped together and 6 dominant pathways were identified (C1 - C6) : 3 eastern pathways, coming from the Atlantic Ocean, and 3 with a western or north-western origin, originating from or passing over the Pacific. In general, at all evaluated height levels the eastern clusters predominate in the frequency of occurrence (approx. 90), which indicates that most of the air masses arriving (Fig. 5) as well as the cluster-concentration statistics (Table3) concur with the occurrence of the highest sodium and chloride concentration between September and February at the most elevated MSs – *El Tiro* and *Cerro del Consuelo* 1000 in the study area originates over the Atlantic. However, even though easterlies prevail, when linking the main transport pathways to the observed concentration at the study site (see Table2)we notice that the easterly trajectories are dominant in terms of frequency of occurrence, but they do not have the greatest impact, considering that they only contribute to small sea-salt concentration. The reason is that the highest concentration is contributed by the Pacific sources in the west and partially by the north-easterlies. Consequently, though the Pacific transport is very sporadic in nature, it contributes to up to 25 of the total concentration at the study area with respect to the analyzed time span between 2004 and 2009. (Fig. 2a, b and Table3). This corroborates the conclusions reached in previous paragraphs that the transport at higher elevations is more synoptically driven. Thus, medium to long-range transport (reproduced by back trajectory modeling) has more of an effect in areas of high elevation than at lower slopes and valleys, which are more affected by local transport.

In order to relate the air mass transportto potential spatial sources of sea-salt

The results of the PSCF and CWT were examined. The results showed that both hypothesized source areas source-receptor models (Fig. 5a, b, c) indicate the areas that contribute to the highest concentration at the receptor site: these areas are , i.e. the equatorial Pacific in the vicinity of the coast of Ecuador and northern Peru as well as the equatorial north-equatorial Atlantic and the

Caribbean sea. Because of the vicinity of the Pacific Ocean Sea. Nonetheless, according to the spatial distribution of the sea salt concentration illustrated in Fig. 8, the PSCF and CWT models seem to overestimate the contribution of the equatorial Pacific, which exhibits a lower sea salt concentration than the Atlantic Ocean. Analysis of the sea salt concentration along the trajectory clusters reveal a comparable behavior, wherein the clusters passing over the Pacific contain a lower sea salt concentration. However, the concentration remains quite stable, contrary to the easterly trajectories passing over the continent, where wet scavenging is much more pronounced. Those drier conditions over the equatorial Pacific were clearly seen in DJF, where the concentration among clusters C4 , the transported aerosols have a lower probability to be scavenged as compared to the long-range transport from the Atlantic over the Amazon. This is most likely the reason why the sources in the Pacific appear stronger and contribute to the highest concentration at C5, and C6 even increase as the air masses approach the receptor site . Comparisons between the selected height levels revealed similar results which point to comparable atmospheric circulation patterns at these altitudes.The best results were gained by the CWT model (Fig. 7).

The CWT (Fig. 7g, h and i) , in successfully allocating 5c) model delivered the best results in that it successfully differentiates the source hot spots over the oceans , distinguishing the hot spots from moderately contribution areas which are sometimes terrestrial. On the contrary from those areas of moderate contribution over the continent. In contrast , the PSCF was (Fig. 5a, b) is less successful in identifying the areas that contributed to the highest concentration making this distinction . As already pointed out reported by Hsu et al. (2003) and Stohl (1996) a drawback of the PSCF method is that the values slightly higher and much higher than high and extreme values above a defined threshold get similar probabilitieswhich complicates , which hamper their distinction. Thus, the results of the PSCF were PSCF results are heavily influenced by the arbitrary choice of the choice of an arbitrary threshold concentration. Pekney et al. (2006) reported that the election selection of the threshold value relies on the evaluated concentration time-series time series . The authors stated found that for low background values and high concentration peaks, the 90th 90^th percentile threshold performs better, while for concentration time-series with less variability, the 75th the 75^th percentile is more appropriate for concentration time series with less variability . In our case, the quite strong seasonal variations in the sea-salt concentration with season explained sea salt concentration explain why the PSCF with 90th percentile threshold performed better than the 75th percentile performed better with the 90^th percentile threshold (Fig. 5b) rather than the 75^th percentile (Fig. 5a) .

Finally, because the general atmospheric circulation and thus, the air mass transport over South America is characterized by a seasonal behaviour which is well documented by in several studies , its effects on the source areas identified by the hybrid receptor models and the clusters associated to these areas was tested (Fig.8 - **??**). Furthermore, seasonal patterns could be observed in the measured

concentration, particularly at the most exposed *Cerro del Consuelo* MS, which highlights its consideration. The quite regular occurrence of the highest concentration between September and February (Fig.3), is in good agreement to the cluster-concentration statistics and the potential sources defined by PSCF and CWT. The highest

To perform a cluster analysis, the trajectories were grouped together and six dominant pathways were identified (C1-C6 in Fig. 6). In general, over the entire observation period, the eastern clusters originating on the equatorial and south-equatorial Atlantic predominate (> 51 % of the trajectories). However, when seasonally linking the main transport pathways (C1-C6) to the sea salt concentration at the receptor site were contributed during SON and DJF (see Fig.**??**). This means that (see Table3), we notice that those pathways do not have the highest impact on the sea salt concentration in southern Ecuador. Even if easterly and south-easterly transport prevail, larger sea salt loads are transported from the largest quantities of sea-salt were transported within this period mainly occurring from the equatorial Pacific and Atlantic. The westerlies are most successful in this period because the ITCZ is located further South north-equatorial Atlantic, the Caribbean Sea, and the equatorial Pacific . The analysis of seasonal patterns in the sea-salt transport strengthen the predominance of air mass transport by eastern trajectories. Moreover, it confirmed that the western trajectories had the strongest impact contributing to the highest sea-salt concentration , because the large quantities were added in a short period of time (only approx 10 The North-Easterlies originating from the north-equatorial Atlantic and Caribbean Sea occurred approximately 29.5 % of the time and accounted for around 56.5 % of the concentration over southern Ecuador. The Westerlies from the equatorial Pacific were much less frequent (≈ 9.3 %of trajectories) , but contributed up to 25) and accounted for 26 % of the total concentration(see Table2) during the analyzed period concentration . That means, despite the barrier effect of the Andes and the low frequency of occurrence occurrences of western pathways, the Pacific sea-salt sources Pacific sea salt sources still play a relevant role in contributing to sea-salt transport to our study site. The comparison of the sodium and chloride concentrationmeasured at our area of investigation with that in other sites located further east substantiates the important role of the Pacific sources at our study area (Table3) . Even if the concentration transporting sea salt to the receptor site. Together, equatorial Pacific and north-equatorial Atlantic sources accounted for around 82.4 % of the total sea salt concentration. Furthermore, large quantities were added solely from the equatorial Pacific and the Caribbean Sea in a short period of time (≈ 16 % of trajectories), contributing up to 46.7 % of the total concentration, which stress the importance of these sources to the atmospheric sea salt budget over southern Ecuador.

Nevertheless, in light of the sea salt concentration along the seasonal trajectory clusters (Fig. 7) and sea salt's spatial distribution (Fig. 8), the significance of Pacific sea salt remains questionable. The concentration of sea salt in the equatorial Pacific is less than that in South Ecuador was not

that high as observed in forests close to the Atlantic, despite the larger distance from the Atlantic coast it clearly exceeded the concentrations measured in the central Brazilian Amazon thousands of kilometers to the east. the Atlantic. Therefore, the former's influence may be overestimated, even if the concentration-decay over the Pacific is much less pronounced as over continental South America. On the one hand, the greater frequency of the North-Easterlies, and on the other hand, the higher sea salt concentration in the Atlantic are good reasons that justify a greater influence of the Caribbean Sea and the north-equatorial Atlantic with respect to the atmospheric sea salt budget over southern Ecuador.

We have used back-trajectory statistical analysis and source-receptor models to assess the allocation and contribution of Pacific and Atlantic Ocean sources to sea-salt (Regarding the addition of salt from biomass-burning to the chloride budget at the study area, based on the co-occurrence of high NO_x concentration from biomass-burning and high sea salt concentration during the main sea salt transport season (SON and DJF, in Figs. 8 and 9), it is very likely that sea salt is indeed enriched by biomass-burning chloride. However, this assumption is not corroborated by our field samples from southern Ecuador. In the concentration of sodium and chloride from rain and OP samples we did not find any correlation between nitrate and sulfate, the products of biomass-burning (Fabian et al., 2009; Makowski Giannoni et al., 2013, 2014)), and sodium and chloride) concentration to our study areain the Andes of South-East Ecuador. As input parameter to the back-trajectory analysis we integrated MACC reanalysis sea-salt concentration (Table2) . As hypothesized, both Atlantic and Pacific sources

Regarding the addition of salt from biomass-burning to the chloride budget at the study area, based on the co-occurrence of high NO_x concentration from biomass-burning and high sea salt concentration during the main sea salt transport season (SON and DJF, in Figs.8 and 9), the enrichment of sea salt with biomass-burning chloride is very likely. However, this assumption is not corroborated by our field samples from South Ecuador. In the concentration of sodium and chloride from rain and OP samples we did not find any correlation between nitrate and sulphate (products of biomass-burning, Fabian et al. (2009); Makowski Giannoni et al. (2013, 2014)), and sodium and chloride (Table2).

6 Conclusions

Sodium and chloride ions exhibited different concentrations in rain and OP along the altitudinal gradient of interest to this study. Their concentration levels and temporal variability in the highest and more exposed MSs presented a stronger seasonality linked to global circulation patterns, and thus a greater influence from sea salt, confirmed by Na^+/Cl^- molar ratios similar to those from marine air masses. Similar seasonal patterns were observed by modeling at a larger scale, using MACC

sea salt concentration data and ERA Interim air mass back-trajectories, confirming the influence of the medium to long-range transport at higher elevations. In contrast, MSs situated at lower altitudes were influenced by the mountain-valley wind systems and local aerosols.

According the sea salt transport analysis by back trajectory modeling for medium to long-range sources, the Caribbean Sea, the north-equatorial Atlantic and equatorial Pacific play an important role to in the transport of sea-salt to the study area in south-eastern Ecuadorat the eastern Andean slopes. The greatest impact was produced by the equatorial Pacific and Atlantic sources and was sea salt to southern Ecuador. Here, the Caribbean and north-equatorial Atlantic sources have the greatest impact. Equatorial Pacific sources, on the other hand, are less significant: It is seasonally driven with the greatest contributions taking place occurring when the ITCZ migrates further south in austral late spring (SON) and summer (DJF)when the ITCZ migrates further South . In total, the Pacific sources only, contributed to up to 25 north-equatorial Atlantic and equatorial Pacific contribute to 56.5 % and 26 % of the total concentration at the study site in southern Ecuador, respectively , which represents an important addition to the total atmospheric sea-salt transport into our study site.Along the examined altitudinal gradient, a difference was observed in terms of the temporal variability of the concentration and its level where the highest and more exposed evaluated station presented a stronger seasonality linked to the large scale circulation. These seasonal patterns were observed in the MACC concentration data as well. The lowermost station was influenced by the mountain-valley winds and the local aerosols transported. Additionally, the higher chloride than sodium concentration and the higher concentration observed at our site in comparison to areas in the central Brazilian Amazon stresses the important role played by the Pacific sources regarding sea-salt transport. sea salt budget.

A comparison of the sodium and chloride concentrations at our area of investigation with those at other sites further east substantiates the important role played by the identified sources (Caribbean Sea, north-equatorial Atlantic, and equatorial Pacific oceans) on the sea salt transport to our study area (Table4). Even if concentrations in southern Ecuador are lower than in forests close to the Atlantic, they clearly exceed those concentrations measured in the central Brazilian Amazon thousands of kilometers to the east, despite being located further from the Atlantic coast. However, whether the higher sodium and chloride availability observed in southern Ecuador makes this tropical ecosystem less salt deprived than other similar ecosystems in the western Amazon is still an open question deserving of investigation.

Appendix A: Tables

Acknowledgements. We thank the German Academic Exchange Service (DAAD) for funding the PhD thesis of S. Makowski Giannoni (Ref. no. A/08/98222) and the German Research Foundation (DFG) for funding this work in the scope of the Research Unit RU816 (funding no. BE 1780/15-1). We are grateful to Giulia F. Curatola Fernández and Tim Appelhans for their valuable help. We also thank the foundation Nature & Culture International (NCI) Loja and San Diego for logistic support.

References

Akagi, S. K., Yokelson, R. J., Wiedinmyer, C., Alvarado, M. J., Reid, J. S., Karl, T., Crounse, J. D., and Wennberg, P. O.: Emission factors for open and domestic biomass burning for use in atmospheric models, Atmos. Chem. Phys., 11, 4039–4072, doi:10.5194/acp-11-4039-2011, http://www.atmos-chem-phys.net/11/4039/2011/, 2011.

Beck, E., Bendix, J., Kottke, I., Makeschin, F., and Mosandl, R., eds.: Gradients in a tropical mountain ecosystem of Ecuador, vol. 198 of *Ecological Studies*, Springer Berlin / Heidelberg, Berlin, Germany, doi:10.1007/978-3-540-73526-7, http://www.springerlink.com/index/10.1007/978-3-540-73526-7, 2008.

Bendix, J., Rollenbeck, R., and Reudenbach, C.: Diurnal patterns of rainfall in a tropical Andean valley of southern Ecuador as seen by a vertically pointing K–band Doppler radar, International Journal of Climatology, 26, 829–846, doi:10.1002/joc.1267, http://onlinelibrary.wiley.com/doi/10.1002/joc.1267/full, 2006.

Bendix, J., Rollenbeck, R., Goettlicher, D., Nauss, T., and Fabian, P.: Seasonality and diurnal pattern of very low clouds in a deeply incised valley of the eastern tropical Andes (South Ecuador) as observed by a cost–effective WebCam system, Meteorological Applications, 15, 281–291, doi:10.1002/met, http://onlinelibrary.wiley.com/doi/10.1002/met.72/abstract, 2008a.

Bendix, J., Rollenbeck, R., Richter, M., Fabian, P., and Emck, P.: Climate, in: Gradients in a Tropical Mountain Ecosystem of Ecuador, edited by Beck, E., Bendix, J., Kottke, I., Makeschin, F., and Mosandl, R., chap. 1, pp. 63–74, Springer Berlin / Heidelberg, ecological edn., http://dx.doi.org/10.1007/978-3-540-73526-7_8, 2008b.

Bendix, J., Beck, E., Brauning, A., Makeschin, F., Mosandl, R., Scheu, S., and Wilcke, W., eds.: Ecosystem services, biodiversity and environmental change in a tropical mountain ecosystem of South Ecuador, vol. xxx, Springer, Berlin-Heidelberg, doi:10.1007/978-3-642-38137-9, http://link.springer.com/book/10.1007%2F978-3-642-38137-9, 2013.

Benedetti, a., Morcrette, J.-J., Boucher, O., Dethof, a., Engelen, R. J., Fisher, M., Flentje, H., Huneeus, N., Jones, L., Kaiser, J. W., Kinne, S., Mangold, a., Razinger, M., Simmons, a. J., and Suttie, M.: Aerosol analysis and forecast in the European Centre for Medium-Range Weather Forecasts Integrated Forecast System: 2. Data assimilation, J. Geophys. Res., 114, D13 205, doi:10.1029/2008JD011115, http://doi.wiley.com/10.1029/2008JD011115, 2009.

Bobbink, R., Hicks, K., and Galloway, J.: Global assessment of nitrogen deposition effects on terrestrial plant diversity: a synthesis, Ecological Applications, 20, 30–59, doi:10.1890/08-1140.1, http://www.esajournals.org/doi/abs/10.1890/08-1140.1, 2010.

Carslaw, D. C. and Ropkins, K.: openair — An R package for air quality data analysis, Environmental Modelling & Software, 27-28, 52–61, doi:10.1016/j.envsoft.2011.09.008, http://linkinghub.elsevier.com/retrieve/pii/S1364815211002064, 2012.

Clarke, N., Zlindra, D., Ulrich, E., Mosello, R., Derome, J., Derome, K., König, N., Lövblad, G., Draaijers, G., Hansen, K., Thimonier, A., and Waldner, P.: sampling and analysis of deposition: Part XIV, in: Manual on methods and criteria for harmonized sampling, assessment, monitoring and analysis of the effects of air pollution on forests., chap. 14, UNECE, ICP Forests, Hamburg, http://icp-forests.net/page/icp-forests-manual, 2010.

Dee, D. P., Uppala, S. M., Simmons, A. J., Berrisford, P., Poli, P., Kobayashi, S., Andrae, U., Balmaseda, M. A., Balsamo, G., Bauer, P., Bechtold, P., Beljaars, A. C. M., van de Berg, L., Bidlot, J., Bormann, N., Delsol, C., Dragani, R., Fuentes, M., Geer, A. J., Haimberger, L., Healy, S. B., Hersbach, H., Hólm, E. V., Isaksen, L., Kållberg, P., Köhler, M., Matricardi, M., McNally, A. P., Monge-Sanz, B. M., Morcrette, J.-J., Park, B.-K., Peubey, C., de Rosnay, P., Tavolato, C., Thépaut, J.-N., and Vitart, F.: The ERA-Interim reanalysis: configuration and performance of the data assimilation system, Q. J. R. Meteorol. Soc., 137, 553–597, doi:10.1002/qj.828, http://doi.wiley.com/10.1002/qj.828, 2011.

Dentener, F., Drevet, J., Lamarque, J. F., Bey, I., Eickhout, B., Fiore, a. M., Hauglustaine, D., Horowitz, L. W., Krol, M., Kulshrestha, U. C., Lawrence, M., Galy-Lacaux, C., Rast, S., Shindell, D., Stevenson, D., Van Noije, T., Atherton, C., Bell, N., Bergman, D., Butler, T., Cofala, J., Collins, B., Doherty, R., Ellingsen, K., Galloway, J., Gauss, M., Montanaro, V., Müller, J. F., Pitari, G., Rodriguez, J., Sanderson, M., Solmon, F., Strahan, S., Schultz, M., Sudo, K., Szopa, S., and Wild, O.: Nitrogen and sulfur deposition on regional and global scales: A multimodel evaluation, Global Biogeochemical Cycles, 20, GB4003, doi:10.1029/2005GB002672, http://dx.doi.org/10.1029/2005GB002672http://www.agu.org/pubs/crossref/2006/2005GB002672.shtml, 2006.

Draxler, R. and Hess, G.: An overview of the HYSPLIT_4 modeling system of trajectories, dispersion, and deposition, Australian Meteorological Magazine, 47, 295–308, 1998.

Dudley, R., Kaspari, M., and Yanoviak, S. P.: Lust for Salt in the Western Amazon, Biotropica, 44, 6–9, doi:10.1111/j.1744-7429.2011.00818.x, http://doi.wiley.com/10.1111/j.1744-7429.2011.00818.x, 2012.

Emck, P.: A climatology of South Ecuador, Phd thesis, University of Erlangen, http://www.opus.ub.uni-erlangen.de/opus/volltexte/2007/656/, 2007.

Fabian, P., Rollenbeck, R., Spichtinger, N., Brothers, L., Dominguez, G., and Thiemens, M.: Sahara dust, ocean spray, volcanoes, biomass burning: pathways of nutrients into Andean rainforests, Advances in Geosciences, 22, 85–94, doi:10.5194/adgeo-22-85-2009, http://www.adv-geosci.net/22/85/2009/, 2009.

Fleming, Z. L., Monks, P. S., and Manning, A. J.: Review: Untangling the influence of air-mass history in interpreting observed atmospheric composition, Atmospheric Research, 104-105, 1–39, doi:10.1016/j.atmosres.2011.09.009, http://linkinghub.elsevier.com/retrieve/pii/S0169809511002948, 2012.

Forti, M. C., Melfi, A. J., Astolfo, R., and Fostier, A.-H.: Rainfall chemistry composition in two ecosystems in the northeastern Brazilian Amazon (Amapá State), Journal of Geophysical Research, 105, 28 895, doi:10.1029/2000JD900235, http://doi.wiley.com/10.1029/2000JD900235, 2000.

Galloway, J. N., Townsend, A. R., Erisman, J. W., Bekunda, M., Cai, Z., Freney, J. R., Martinelli, L. a., Seitzinger, S. P., and Sutton, M. a.: Transformation of the nitrogen cycle: recent trends, questions, and potential solutions., Science (New York, N.Y.), 320, 889–92, doi:10.1126/science.1136674, http://www.ncbi.nlm.nih.gov/pubmed/18487183, 2008.

Griffith, K. T., Ponette-González, A. G., Curran, L. M., and Weathers, K. C.: Assessing the influence of topography and canopy structure on Douglas fir throughfall with LiDAR and empirical data in the Santa Cruz mountains, USA., Environmental monitoring and assessment, 187, 4486, doi:10.1007/s10661-015-4486-6, http://www.ncbi.nlm.nih.gov/pubmed/25893759, 2015.

Guelle, W., Schulz, M., Balkanski, Y., and Dentener, F.: Influence of the source formulation on modeling the atmospheric global distribution of sea salt aerosol, Journal of Geophysical Research, 106, 27 509, doi:10.1029/2001JD900249, http://doi.wiley.com/10.1029/2001JD900249, 2001.

Harrison, R. M. and Pio, C. A.: Major ion composition and chemical associations of inorganic atmospheric aerosols., Environmental science & technology, 17, 169–74, doi:10.1021/es00109a009, http://dx.doi.org/10.1021/es00109a009, 1983.

Hildemann, L. M., Markowski, G. R., and Cass, G. R.: Chemical composition of emissions from urban sources of fine organic aerosol, Environmental Science & Technology, 25, 744–759, doi:10.1021/es00016a021, http://dx.doi.org/10.1021/es00016a021, 1991.

Homeier, J., Hertel, D., Camenzind, T., Cumbicus, N. L., Maraun, M., Martinson, G. O., Poma, L. N., Rillig, M. C., Sandmann, D., Scheu, S., Veldkamp, E., Wilcke, W., Wullaert, H., and Leuschner, C.: Tropical andean forests are highly susceptible to nutrient inputs-rapid effects of experimental N and p addition to an ecuadorian montane forest., PloS one, 7, e47 128, doi:10.1371/journal.pone.0047128, http://www.pubmedcentral.nih.gov/articlerender.fcgi?artid=3468540&tool=pmcentrez&rendertype=abstract, 2012.

Hsu, Y.-K., Holsen, T. M., and Hopke, P. K.: Comparison of hybrid receptor models to locate PCB sources in Chicago, Atmospheric Environment, 37, 545–562, doi:10.1016/S1352-2310(02)00886-5, http://linkinghub.elsevier.com/retrieve/pii/S1352231002008865, 2003.

Inness, A., Baier, F., Benedetti, A., Bouarar, I., Chabrillat, S., Clark, H., Clerbaux, C., Coheur, P., Engelen, R. J., Errera, Q., Flemming, J., George, M., Granier, C., Hadji-Lazaro, J., Huijnen, V., Hurtmans, D., Jones, L., Kaiser, J. W., Kapsomenakis, J., Lefever, K., Leitão, J., Razinger, M., Richter, A., Schultz, M. G., Simmons, A. J., Suttie, M., Stein, O., Thépaut, J.-N., Thouret, V., Vrekoussis, M., and Zerefos, C.: The MACC reanalysis: an 8 yr data set of atmospheric composition, Atmos. Chem. Phys., 13, 4073–4109, doi:10.5194/acp-13-4073-2013, http://www.atmos-chem-phys.net/13/4073/2013/, 2013.

Jaeglé, L., Quinn, P. K., Bates, T. S., Alexander, B., and Lin, J.-T.: Global distribution of sea salt aerosols: new constraints from in situ and remote sensing observations, Atmospheric Chemistry and Physics, 11, 3137–3157, doi:10.5194/acp-11-3137-2011, http://www.atmos-chem-phys.net/11/3137/2011/acp-11-3137-2011.html, 2011.

Kaiser, J. W., Heil, A., Andreae, M. O., Benedetti, A., Chubarova, N., Jones, L., Morcrette, J.-J., Razinger, M., Schultz, M. G., Suttie, M., and van der Werf, G. R.: Biomass burning emissions estimated with a global fire assimilation system based on observed fire radiative power, Biogeosciences, 9, 527–554, doi:10.5194/bg-9-527-2012, http://www.biogeosciences.net/9/527/2012/, 2012.

Kaspari, M., Yanoviak, S. P., and Dudley, R.: On the biogeography of salt limitation: a study of ant communities., Proceedings of the National Academy of Sciences of the United States of America, 105, 17 848–51, doi:10.1073/pnas.0804528105, http://www.pubmedcentral.nih.gov/articlerender.fcgi?artid=2584704&tool=pmcentrez&rendertype=abstract, 2008.

Kaspari, M., Yanoviak, S. P., Dudley, R., Yuan, M., and Clay, N. A.: Sodium shortage as a constraint on the carbon cycle in an inland tropical rainforest., Proceedings of the National Academy of Sciences of the United States of America, 106, 19 405–9, doi:10.1073/pnas.0906448106, http://www.pnas.org/content/106/46/19405.abstract, 2009.

Keene, W. C., Pszenny, A. A. P., Galloway, J. N., and Hawley, M. E.: Sea-salt corrections and interpretation of constituent ratios in marine precipitation, Journal of Geophysical Research, 91, 6647, doi:10.1029/JD091iD06p06647, http://doi.wiley.com/10.1029/JD091iD06p06647, 1986.

Kirchner, M., Fegg, W., Römmelt, H., Leuchner, M., Ries, L., Zimmermann, R., Michalke, B., Wallasch, M., Maguhn, J., Faus-Kessler, T., and Jakobi, G.: Nitrogen deposition along differently exposed slopes in the Bavarian Alps., The Science of the total environment, 470-471, 895–906, doi:10.1016/j.scitotenv.2013.10.036, http://www.sciencedirect.com/science/article/pii/S0048969713011807, 2014.

Koehler, B., Corre, M. D., Veldkamp, E., Wullaert, H., and Wright, S. J.: Immediate and long-term nitrogen oxide emissions from tropical forest soils exposed to elevated nitrogen input, Global Change Biology, 15, 2049–2066, doi:10.1111/j.1365-2486.2008.01826.x, http://doi.wiley.com/10.1111/j.1365-2486.2008.01826.x, 2009.

Lee, A. T. K., Kumar, S., Brightsmith, D. J., and Marsden, S. J.: Parrot claylick distribution in South America: do patterns of "where" help answer the question "why"?, Ecography, doi:10.1111/j.1600-0587.2009.05878.x, http://doi.wiley.com/10.1111/j.1600-0587.2009.05878.x, 2009.

Lizcano, D. J. and Cavelier, J.: Características Químicas de salados y hábitos alimenticios de la Danta de montaña (Tapirus pinchaque Roulin, 1829) en los Andes Centrales de Colombia, Mastozoología neotropical, 11, 193–201, http://www.scielo.org.ar/scielo.php?script=sci_arttext&pid=S0327-93832004000200004&lng=es&nrm=iso&tlng=es, 2004.

Lovett, G. and Kinsman, J.: Atmospheric pollutant deposition to high-elevation ecosystems, Atmospheric Environment. Part A. General Topics, 24, 2767–2786, http://www.sciencedirect.com/science/article/pii/096016869090164I, 1990.

Mahowald, N. M., Artaxo, P., Baker, A. R., Jickells, T. D., Okin, G. S., Randerson, J. T., and Townsend, A. R.: Impacts of biomass burning emissions and land use change on Amazonian atmospheric phosphorus cycling and deposition, Global Biogeochem. Cycles, 19, n/a–n/a, doi:10.1029/2005GB002541, http://doi.wiley.com/10.1029/2005GB002541, 2005.

Makowski Giannoni, S., Rollenbeck, R., Fabian, P., and Bendix, J.: Complex topography influences atmospheric nitrate deposition in a neotropical mountain rainforest, Atmospheric Environment, 79, 385–394, doi:10.1016/j.atmosenv.2013.06.023, http://www.sciencedirect.com/science/article/pii/S1352231013004780http://linkinghub.elsevier.com/retrieve/pii/S1352231013004780, 2013.

Makowski Giannoni, S., Rollenbeck, R., Trachte, K., and Bendix, J.: Natural or anthropogenic? On the origin of atmospheric sulfate deposition in the Andes of southeastern Ecuador, Atmospheric Chemistry and Physics, 14, 11 297–11 312, doi:10.5194/acp-14-11297-2014, http://www.atmos-chem-phys.net/14/11297/2014/acp-14-11297-2014.html, 2014.

Malm, W. C., Johnson, C. E., and Bresch, J. F.: Application of principal component analysis for purposes of identifying source-receptor relationships, in: Receptor methods for source apportionment, edited by Pace, T. G., Air pollution control association, Pittsburgh, PA, 1986.

Matson, A. L., Corre, M. D., and Veldkamp, E.: Nitrogen cycling in canopy soils of tropical montane forests responds rapidly to indirect N and P fertilization., Global change biology, 20, 3802–13, doi:10.1111/gcb.12668, http://www.ncbi.nlm.nih.gov/pubmed/24965673, 2014.

Matson, P., Lohse, K. A., and Hall, S. J.: The Globalization of Nitrogen Terrestrial Deposition : Ecosystems Consequences for, Ambio, 31, 2002.

Millero, F.: Treatise on Geochemistry, Elsevier, doi:10.1016/B978-0-08-095975-7.00601-X, http://www.sciencedirect.com/science/article/pii/B978008095975700601X, 2014.

Morcrette, J.-J., Boucher, O., Jones, L., Salmond, D., Bechtold, P., Beljaars, a., Benedetti, a., Bonet, a., Kaiser, J. W., Razinger, M., Schulz, M., Serrar, S., Simmons, a. J., Sofiev, M., Suttie, M., Tompkins, a. M., and Untch, a.: Aerosol analysis and forecast in the European Centre for Medium-Range Weather Forecasts Integrated Forecast System: Forward modeling, Journal of Geophysical Research, 114, D06 206, doi:10.1029/2008JD011235, http://doi.wiley.com/10.1029/2008JD011235, 2009.

Mortatti, J.: Erosão na Amazonia: processos. Modelos e balanço, Ph.D. thesis, São Paulo, Brazil, 1995.

Pauliquevis, T., Lara, L. L., Antunes, M. L., and Artaxo, P.: Aerosol and precipitation chemistry measurements in a remote site in Central Amazonia: the role of biogenic contribution, Atmospheric Chemistry and Physics, 12, 4987–5015, doi:10.5194/acp-12-4987-2012, http://www.atmos-chem-phys.net/12/4987/2012/acp-12-4987-2012.html, 2012.

Pekney, N. J., Davidson, C. I., Zhou, L., and Hopke, P. K.: Application of PSCF and CPF to PMF-Modeled Sources of PM 2.5 in Pittsburgh, Aerosol Science and Technology, 40, 952–961, doi:10.1080/02786820500543324, http://www.tandfonline.com/doi/abs/10.1080/02786820500543324, 2006.

Peñuelas, J., Poulter, B., Sardans, J., Ciais, P., van der Velde, M., Bopp, L., Boucher, O., Godderis, Y., Hinsinger, P., Llusia, J., Nardin, E., Vicca, S., Obersteiner, M., and Janssens, I. A.: Human-induced nitrogen-phosphorus imbalances alter natural and managed ecosystems across the globe., Nat. Commun., 4, 2934, doi:10.1038/ncomms3934, http://www.nature.com/ncomms/2013/131217/ncomms3934/full/ncomms3934.html, 2013.

Pett-Ridge, J. C.: Contributions of dust to phosphorus cycling in tropical forests of the Luquillo Mountains, Puerto Rico, Biogeochemistry, 94, 63–80, doi:10.1007/s10533-009-9308-x, http://link.springer.com/10.1007/s10533-009-9308-x, 2009.

Phoenix, G. K., Hicks, K. W., Cinderby, S., Kuylenstierna, J. C. I., Stock, W. D., Dentener, F. J., Giller, K. E., Austin, A. T., Lefroy, R. D. B., Gimeno, B. S., Ashmore, M. R., and Ineson, P.: Atmospheric nitrogen deposition in world biodiversity hotspots: the need for a greater global perspective in assessing N deposition impacts, Global Change Biology, 12, 470–476, doi:10.1111/j.1365-2486.2006.01104.x, http://dx.doi.org/10.1111/j.1365-2486.2006.01104.x, 2006.

Powell, L. L., Powell, T. U., Powell, G. V. N., and Brightsmith, D. J.: Parrots Take it with a Grain of Salt: Available Sodium Content May Drive Collpa (Clay Lick) Selection in Southeastern Peru, Biotropica, 41, 279–282, doi:10.1111/j.1744-7429.2009.00514.x, http://doi.wiley.com/10.1111/j.1744-7429.2009.00514.x, 2009.

Pozzer, a., de Meij, a., Pringle, K. J., Tost, H., Doering, U. M., van Aardenne, J., and Lelieveld, J.: Distributions and regional budgets of aerosols and their precursors simulated with the EMAC chemistry-climate model, Atmospheric Chemistry and Physics, 12, 961–987, doi:10.5194/acp-12-961-2012, http://www.atmos-chem-phys.net/12/961/2012/, 2012.

Reid, J. S., Prins, E. M., Westphal, D. L., Schmidt, C. C., Richardson, K. A., Christopher, S. A., Eck, T. F., Reid, E. A., Curtis, C. A., and Hoffman, J. P.: Real-time monitoring of South American smoke particle emissions and transport using a coupled remote sensing/box-model approach, Geophys. Res. Lett., 31, n/a–n/a, doi:10.1029/2003GL018845, http://doi.wiley.com/10.1029/2003GL018845, 2004.

Richter, M., Beck, E., Rollenbeck, R., and Bendix, J.: The study area, in: Ecosystemservices, biodiversity and environmental change in a tropical mountain ecosystem of South Ecuador, edited by Bendix, J., Beck, E., Brauning, A., Makeschin, F., Mosandl, R., Scheu, S., and Wilcke, W., chap. 1, Springer Berlin / Heidelberg, Berlin, Germany, doi:10.1007/978-3-642-38137-9_1, http://link.springer.com/chapter/10.1007/978-3-642-38137-9_1, 2013.

Riuttanen, L., Hulkkonen, M., Dal Maso, M., Junninen, H., and Kulmala, M.: Trajectory analysis of atmospheric transport of fine particles, SO₂, NO_x and O₃ to the SMEAR II station in Finland in 1996–2008, Atmospheric Chemistry and Physics, 13, 2153–2164, doi:10.5194/acp-13-2153-2013, http://www.atmos-chem-phys.net/13/2153/2013/, 2013.

Robinson, N. H., Newton, H. M., Allan, J. D., Irwin, M., Hamilton, J. F., Flynn, M., Bower, K. N., Williams, P. I., Mills, G., Reeves, C. E., McFiggans, G., and Coe, H.: Source attribution of Bornean air masses by back trajectory analysis during the OP3 project, Atmospheric Chemistry and Physics, 11, 9605–9630, doi:10.5194/acp-11-9605-2011, http://www.atmos-chem-phys.net/11/9605/2011/acp-11-9605-2011.html, 2011.

Rollenbeck, R., Bendix, J., Fabian, P., Boy, J., Wilcke, W., Dalitz, H., Oesker, M., and Emck, P.: Comparison of different techniques for the measurement of precipitation in tropical montane rain forest regions, Journal of Atmospheric and Oceanic Technology, 24, 156–168, doi:10.1175/JTECH1970.1, http://journals.ametsoc.org/doi/abs/10.1175/JTECH1970.1, 2007.

Rollenbeck, R., Bendix, J., and Fabian, P.: Spatial and temporal dynamics of atmospheric water inputs in tropical mountain forests of South Ecuador, Hydrological Processes, 25, 344–352, doi:10.1002/hyp.7799, http://doi.wiley.com/10.1002/hyp.7799, 2011.

Schemenauer, R. S. and Cereceda, P.: A proposed standard fog collector for use in high-elevation regions, Journal of Applied Meteorology, 33, 1313–1322, http://adsabs.harvard.edu/abs/1994JApMe..33.1313S, 1994.

Schulz, M., de Leeuw, G., and Balkanski, Y.: Sea-salt aerosol source functions and emissions, in: Emissions of Atmospheric Trace Compounds, pp. 333–359, Springer Netherlands, doi:10.1007/978-1-4020-2167-1_9, http://link.springer.com/chapter/10.1007/978-1-4020-2167-1_9, 2004.

Seibert, P., Kromb-Kolb, H., Baltensperger, U., Jost, D., and Schwikowski, M.: Trajectory analysis of high-alpine air pollution data, in: NATO challenges of modern society, edited by Gryning, S.-E. and Millán, M. M., pp. 595–596, Springer US, doi:10.1007/978-1-4615-1817-4_65, http://link.springer.com/chapter/10.1007/978-1-4615-1817-4_65, 1994.

Spanos, T.: Environmetric modeling of emission sources for dry and wet precipitation from an urban area, Talanta, 58, 367–375, doi:10.1016/S0039-9140(02)00285-0, http://www.sciencedirect.com/science/article/pii/S0039914002002850, 2002.

Stohl, A.: Trajectory statistics-A new method to establish source-receptor relationships of air pollutants and its application to the transport of particulate sulfate in Europe, Atmospheric Environment, 30, 579–587, doi:10.1016/1352-2310(95)00314-2, http://linkinghub.elsevier.com/retrieve/pii/1352231095003142, 1996.

Talbot, R. W., Andreae, M. O., Berresheim, H., Artaxo, P., Garstang, M., Harriss, R. C., Beecher, K. M., and Li, S. M.: Aerosol Chemistry During the Wet Season in Central Amazonia: The Influence of Long-Range Transport, J. Geophys. Res., 95, 16 955–16 969, http://dx.doi.org/10.1029/JD095iD10p16955, 1990.

Tanner, E. V. J., Vitousek, P. M., and Cuevas, E.: Experimental investigation of nutrient limitation of forest growth on wet tropical mountains, Ecology, 79, 10–22, doi:10.1890/0012-9658(1998)079[0010:EIONLO]2.0.CO;2, http://www.esajournals.org/doi/abs/10.1890/0012-9658(1998)079[0010:EIONLO]2.0.CO;2, 1998.

Tardy, Y., Bustillo, V., Roquin, C., Mortatti, J., and Victoria, R.: The Amazon. Bio-geochemistry applied to river basin management, Applied Geochemistry, 20, 1746–1829, doi:10.1016/j.apgeochem.2005.06.001, http://linkinghub.elsevier.com/retrieve/pii/S0883292705001113, 2005.

Tipping, E., Benham, S., Boyle, J. F., Crow, P., Davies, J., Fischer, U., Guyatt, H., Helliwell, R., Jackson-Blake, L., Lawlor, a. J., Monteith, D. T., Rowe, E. C., and Toberman, H.: Atmospheric deposition of phosphorus to land and freshwater., Environ. Sci. Process. Impacts, 16, 1608–17, doi:10.1039/c3em00641g, http://www.ncbi.nlm.nih.gov/pubmed/24526176, 2014.

Vet, R., Artz, R. S., Carou, S., Shaw, M., Ro, C.-U., Aas, W., Baker, A., Bowersox, V. C., Dentener, F., Galy-Lacaux, C., Hou, A., Pienaar, J. J., Gillett, R., Forti, M. C., Gromov, S., Hara, H., Khodzher, T., Mahowald, N. M., Nickovic, S., Rao, P., and Reid, N. W.: A global assessment of precipitation chemistry and deposition of sulfur, nitrogen, sea salt, base cations, organic acids, acidity and pH, and phosphorus, Atmospheric Environment, 93, 3–100, doi:10.1016/j.atmosenv.2013.10.060, http://www.sciencedirect.com/science/article/pii/S1352231013008133, 2014.

Vitousek, P. M.: Litterfall, Nutrient Cycling, and Nutrient Limitation in Tropical Forests, 65, 285–298, http://www.esajournals.org/doi/abs/10.2307/1939481, 1984.

Voigt, C. C., Capps, K. A., Dechmann, D. K. N., Michener, R. H., and Kunz, T. H.: Nutrition or detoxification: why bats visit mineral licks of the Amazonian rainforest., PloS one, 3, e2011, doi:10.1371/journal.pone.0002011, http://journals.plos.org/plosone/article?id=10.1371/journal.pone.0002011, 2008.

Wang, F., Li, J., Wang, X., Zhang, W., Zou, B., Neher, D. A., and Li, Z.: Nitrogen and phosphorus addition impact soil N2O emission in a secondary tropical forest of South China., Scientific reports, 4, 5615, doi:10.1038/srep05615, http://www.nature.com/srep/2014/140708/srep05615/full/srep05615.html, 2014.

Wilcke, W., Leimer, S., Peters, T., Emck, P., Rollenbeck, R., Trachte, K., Valarezo, C., and Bendix, J.: The nitrogen cycle of tropical montane forest in Ecuador turns inorganic under environmental change, Global Biogeochemical Cycles, 27, 1194–1204, doi:10.1002/2012GB004471, http://doi.wiley.com/10.1002/2012GB004471, 2013.

Williams, M. R., Fisher, T. R., and Melack, J. M.: Chemical composition and deposition of rain in the central Amazon, Brazil, Atmospheric Environment, 31, 207–217, doi:10.1016/1352-2310(96)00166-5, http://www.sciencedirect.com/science/article/pii/1352231096001665, 1997.

Wolf, K., Veldkamp, E., Homeier, J., and Martinson, G. O.: Nitrogen availability links forest productivity, soil nitrous oxide and nitric oxide fluxes of a tropical montane forest in southern Ecuador, Global Biogeochemical Cycles, 25, GB4009, doi:10.1029/2010GB003876, http://www.agu.org/pubs/crossref/2011/2010GB003876.shtml, 2011.

Wullaert, H., Geographie, P., Chemie, F., and Gutenberg-universit, J.: Response of nutrient cycles of an old-growth montane forest in Ecuador to experimental low-level nutrient amendments, Ph.D. thesis, http://ubm.opus.hbz-nrw.de/volltexte/2010/2312/, 2010.

Yokouchi, Y., Ikeda, M., Inuzuka, Y., and Yukawa, T.: Strong emission of methyl chloride from tropical plants., Nature, 416, 163–5, doi:10.1038/416163a, http://dx.doi.org/10.1038/416163a, 2002.

Yu, H., Chin, M., Yuan, T., Bian, H., Remer, L. A., Prospero, J. M., Omar, A., Winker, D., Yang, Y., Zhang, Y., Zhang, Z., and Zhao, C.: The Fertilizing Role of African Dust in the Amazon Rainforest: A First Multiyear Assessment Based on CALIPSO Lidar Observations, Geophysical Research Letters, pp. n/a–n/a, doi:10.1002/2015GL063040, http://doi.wiley.com/10.1002/2015GL063040, 2015.

Zeng, Y. and Hopke, P.: A study of the sources of acid precipitation in Ontario, Canada, Atmospheric Environment (1967), 23, 1499–1509, doi:10.1016/0004-6981(89)90409-5, http://www.sciencedirect.com/science/article/pii/0004698189904095, 1989.

We thank the German Academic Exchange Service (DAAD) for funding the PhD thesis of S. Makowski Giannoni (Ref. no. A/08/98222) and the German Research Foundation (DFG) for the funding of the work in the scope of the Research Unit RU816 (funding no. BE 1780/15-1). We are grateful to Giulia F. Curatola Fernández and Tim Appelhans for their valuable help. We also thank the foundation Nature Culture International (NCI)Loja and San Diego for logistic support.

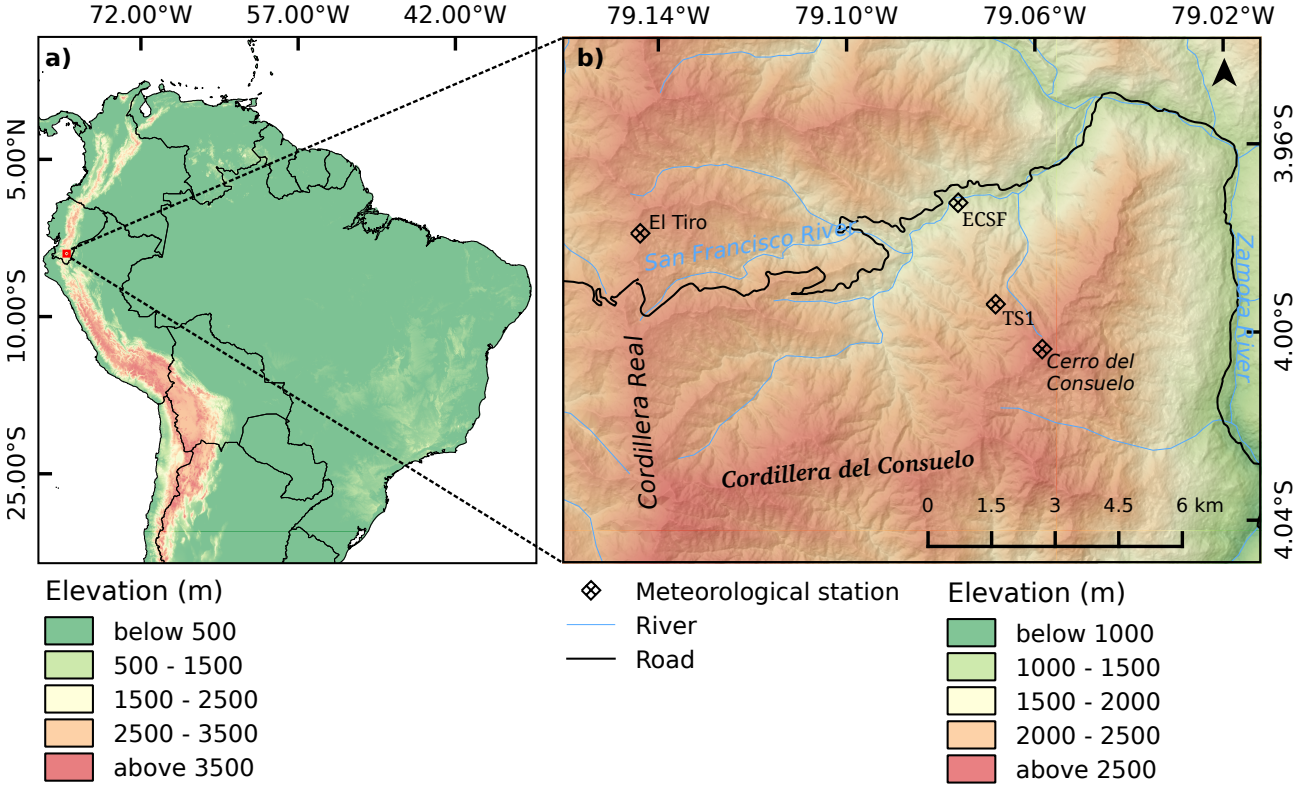

Figure 1. Map of the study area. a) Location of the study area in the Huancabamba depression of the Andes in South-America South America . b) Detailed map of the rain and occult precipitation (OP) sampling sites installed in the study area.

Table A1. Average ion concentration in rain and occult precipitation (OP), precipitation volume, and electrical conductivity at meteorological stations (MSs) along an altitudinal gradient.

site	collector	elev (meters)	P (mm)	pH	eC ($\mu S.cm^{-1}$)	NH_4^-	Ca^+	Cl^-	PO_4^-	Mg^+ ($mg.l_{-1}$)	NO_3^-	K^+	Na^+	SO_4^-
C. del Consuelo	OP	3180	1.1e+02	5.4	12	0.55	0.17	0.42	0.085	0.059	0.82	0.15	0.22	1
C. del Consuelo	Rain	3180	4.7e+02	5.3	3.5	0.18	0.1	0.29	0.16	0.05	0.11	0.098	0.14	0.26
ECSF	OP	1960	7.3	5	13	0.17	0.42	0.86	0.098	0.073	0.14	0.23	0.22	0.44
ECSF	Rain	1960	1.4e+02	5.3	4.3	0.15	0.11	0.43	0.13	0.048	0.077	0.16	0.18	0.24
El Tiro	OP	2825	75	6	20	0.8	0.19	0.45	0.12	0.07	1.4	0.3	0.31	1.6
El Tiro	Rain	2825	1.4e+02	5.4	5.4	0.22	0.14	0.36	0.15	0.047	0.12	0.15	0.24	0.39
TS1	OP	2660	34	5.3	5.2	0.25	0.12	0.5	0.16	0.054	0.16	0.12	0.25	0.32
TS1	Rain	2660	2.8e+02	5.4	4	0.18	0.077	0.36	0.13	0.047	0.084	0.13	0.18	0.26

Table 1. Results from the correlation analysis between sea-salt sea salt monthly mean concentration from Monitoring Atmospheric Composition and Climate (MACC) reanalysis data and Na^+ and Cl^- monthly mean concentration samples from *El Tiro* and *Cerro del Consuelo* meteorological station (MS) samples stations . Correlation was Correlations were tested for the different height levels of various elevations within the MACC data set dataset .

	MACC1 (0.03-0.5 μm)			MACC2 (0.5-5 μm)			MACC3 (5-20 μm)		
	Cl^-	Na^+	mean	Cl^-	Na^+	mean	Cl^-	Na^+	mean
Cerro del Consuelo									
700 hPa	0-.36**	0.35**	0.18	0.52***	0.52***	0.40***	0.48***	0.47***	0.52***
600 hPa	0.31**	0.26*	0.1	0.50***	0.47***	0.39**	0.36**	0.30*	0.40***
500 hPa	0.27*	0.19	0.03	0.47***	0.36**	0.30*	0.22	0.13	0.28*
400 hPa	0.24*	0.19	0.03	0.37**	0.27*	0.23	0.08	0.02	0.17
300 hPa	0.11	0.02	-0.05	0.25*	0.16	0.23	0.01	-0.05	0.14
200 hPa	0.22	0.09	0.03	0.30*	0.18	0.25*	-0.02	-0.04	0.08
El Tiro									
700 hPa	0.34**	0.18	0.18	0.41***	0.17	0.2	0.32**	0.05	0.16
600 hPa	0.37**	0.22	0.2	0.40***	0.14	0.18	0.19	-0.08	0.07
500 hPa	0.33**	0.18	0.16	0.31**	0.05	0.09	0.02	-0.15	-0.04
400 hPa	0.24*	0.14	0.12	0.14	-0.02	0	-0.14	-0.16	-0.12
300 hPa	0.14	0.15	0.1	-0.01	-0.08	-0.05	-0.21	-0.15	-0.13
200 hPa	0.15	0.15	0.19	-0.01	-0.12	0.01	-0.17	0.01	-0.04

note:* p<0.05, ** p<0.01, *** p<0.001

Table 2. Loadings from principal factor analysis (PFA) with varimax rotation of major ions in rain and occult precipitation (OP) samples from *Cerro del Consuelo*, *El Tiro*, TS1, and ECSF meteorological stations.

	Rain				Occult precipitation (OP)			
	Factor1	Factor2	Factor3	Factor4	Factor1	Factor2	Factor3	Factor4
				Cerro del Consuelo				
NH_4^+	0.05	0.14	0.81	0.00	0.88	0.09	0.15	0.08
Ca^{2+}	0.05	0.08	-0.04	0.73	0.17	0.30	0.60	0.60
Cl^-	0.88	0.44	0.06	-0.15	0.23	0.81	0.13	0.35
Mg^{2+}	0.04	-0.21	0.70	-0.06	0.17	0.20	0.86	0.14
NO_3^-	0.27	0.91	0.00	0.19	0.87	0.27	-0.02	0.42
K^+	0.85	0.06	-0.02	0.28	0.84	0.24	0.25	0.09
Na^+	0.88	0.37	0.19	-0.00	0.19	0.83	0.24	0.05
SO_4^{2-}	0.49	0.64	-0.15	-0.03	0.54	0.30	0.34	0.64
				El Tiro				
NH_4^+	-0.07	-0.06	0.64	0.03	0.82	0.34	0.28	0.22
Ca^{2+}	-0.02	0.11	0.03	0.40	0.34	0.29	0.68	0.09
Cl^-	0.98	0.09	-0.11	-0.11	0.31	0.90	0.25	0.01
Mg^{2+}	0.05	-0.04	0.87	-0.03	0.48	0.38	0.52	0.38
NO_3^-	-0.06	0.80	-0.18	0.20	0.81	0.38	0.38	0.08
K^+	0.15	0.42	0.35	-0.38	0.85	0.30	0.39	0.02
Na^+	0.97	0.04	0.08	0.01	0.33	0.87	0.31	0.16
SO_4^{2-}	0.13	0.84	-0.00	0.08	0.61	0.32	0.63	-0.02
				TS1				
NH_4^+	-0.04	0.05	0.59	0.27	0.03	0.12	0.09	0.68
Ca^{2+}	-0.06	-0.16	-0.02	0.04	0.67	0.23	0.37	0.21
Cl^-	0.36	0.89	-0.15	0.04	0.89	0.37	0.16	-0.00
Mg^{2+}	-0.22	-0.09	0.78	0.04	0.45	-0.15	0.55	0.46
NO_3^-	0.91	0.14	-0.20	0.27	0.22	0.89	0.00	0.18
K^+	0.15	0.08	0.34	0.67	0.57	0.42	0.58	0.18
Na^+	-0.04	0.89	-0.00	0.33	0.91	0.35	0.19	0.07
SO_4^{2-}	0.83	0.29	-0.11	-0.06	0.41	0.80	0.13	0.00
				ECSF				
NH_4^+	0.01	0.78	0.11	-0.10	0.34	0.42	0.39	0.43
Ca^{2+}	0.23	0.01	0.02	0.03	-0.04	0.03	0.07	0.50
Cl^-	0.49	-0.23	0.04	0.30	0.31	0.77	0.34	0.32
Mg^{2+}	-0.10	0.54	-0.59	0.09	0.05	0.33	0.73	0.23
NO_3^-	-0.00	0.22	0.75	0.31	0.80	0.07	0.01	0.01
K^+	0.65	-0.02	-0.10	0.03	0.52	0.37	0.64	0.04
Na^+	0.80	0.02	0.15	0.22	0.13	0.79	0.25	-0.02
SO_4^{2-}	0.24	-0.07	0.17	0.73	0.77	0.29	0.27	-0.03

Table 3. Mean sea-salt sea salt concentration and percentage of total concentration for each season at the receptor site in the Andes of south-eastern Ecuador associated to each the mean trajectory cluster clusters (C1-C6) for in the considered height levels Andes of southern Ecuador . The percentage contribution of the mean clusters to the total concentration is shown in parenthesis.

	3180 m C1	4200 m C2	6000 m C3
C1 Summer (DJF)	1.33 5.12 E-09(30.32 14.42)	1.41 5.18 E-09(28.39 43.76)	7.53E-10 (30.93) C2 3.81E-09(22.99)
C3 Autumn (MAM)	1.93 1.90 E-09(8.53 30.34)	6.46E-10 (24.48 3.80E-09(36.42)	1.49 1.35 E-09(7.44) C4 17.6)
C5 Winter (JJA)	2.01 1.72 E-09(9.17 21.28)	2.37 1.83 E-09(6.60 24.33)	1.17 1.64 E-09(26.02 3.2)
C6 Spring (SON)	6.67E-10 (21.18 2.16E-09(23.63)	1.96 2.33 E-09(7.65 28.36)	1.79 2.70 E-09(5.68 17.77)

Table 4. Comparison of the mean concentration of Na^+ and Cl^- mean concentration in precipitation in this study with data from other sites in the Amazon basin. The values represent Volume Weighted Means expressed in μeq l^{-1}.

	Na^+	Cl^-	Reference
South Ecuador (RBSF)	7.80	9.60	This study
Central Amazon (Manaus) 7.78 7.70 Central Amazon (Lake Calado)	2.40	4.60	Williams et al. (1997)
Central Amazon (Balbina)	3.80	5.20	Pauliquevis et al. (2012)
Northeast Amazon	16.60	16.90	Forti et al. (2000)
Eastern Amazon (Belem)	18.90	19.50	Mortatti (1995)

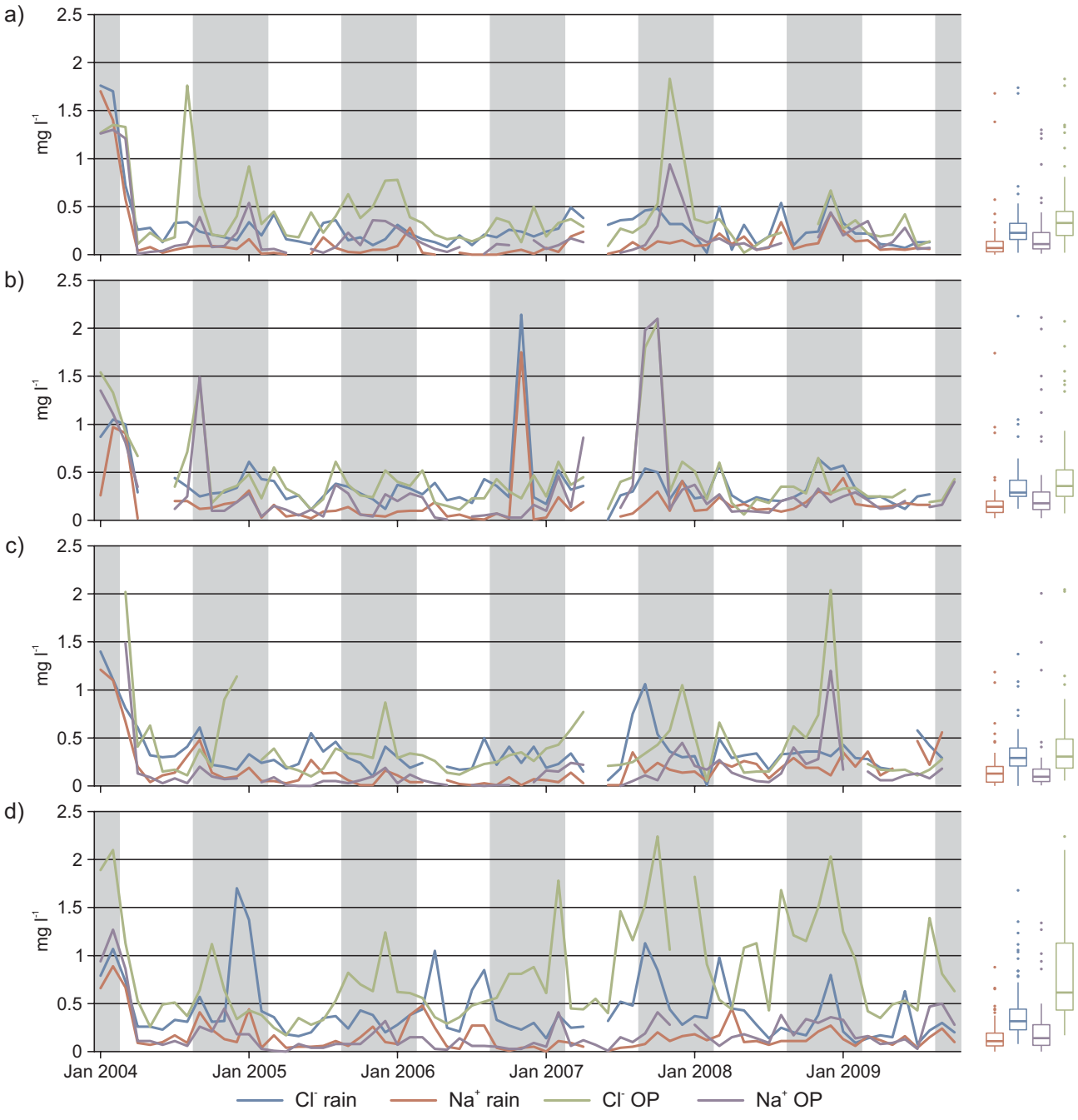

Figure 2. Time-series Time series of Na^+ and Cl^- volume weighted monthly mean (VWMM) concentration in rain and occult precipitation (OP). These samples come from meteorological stations (MSs) at different altitudes and topographical locations: a) *Cerro del Consuelo* (3180 m), b) *El Tiro* (2825 m), c) TS1 (2660 m), and d) ECSF (1960 m). The shaded areas cover 6 months six-month periods from September to February. The box plots on in the right column show the distribution of each time-series. The boxes time series: Boxes symbolize the lower and upper quartile of the data. Vertical , vertical lines show ranges of observed concentration and points are outliers.

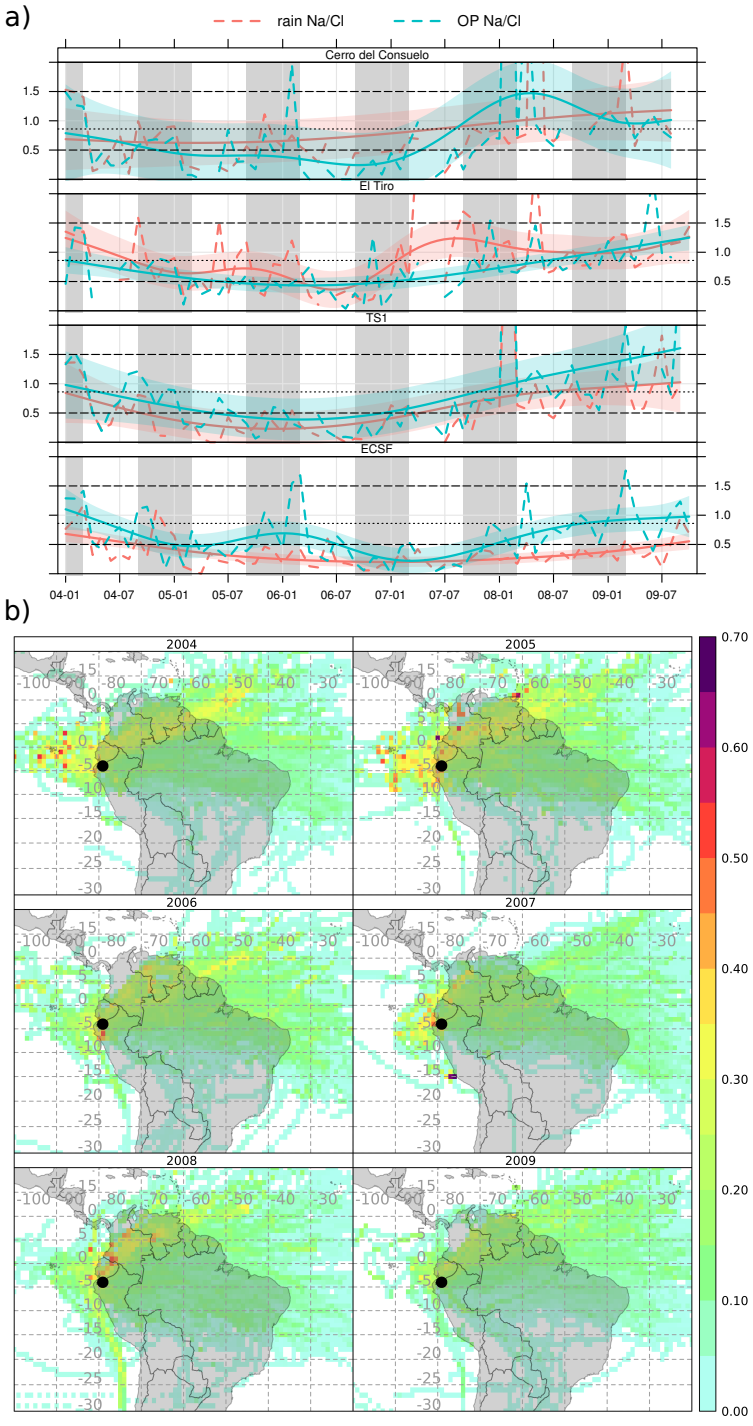

Figure 3. Factor analysis with varimax rotation of major ions in rain (in blue) and occult precipitation (OP, in red) samples from a) *Cerro del Consuelo*, b) *El Tiro*, c) TS1, and d) ECSF Time series of monthly Na^{+}/Cl^{-} molar ratios for the four meteorological stations (MSs) . The bottom x axis represents the resulting factors; the upper x axis shows along the explained variability; altitudinal gradient. Smooth lines are fitted as solid lines and the y axis represents 95 % confidence interval is shown by the loadings shaded area. b) Yearly concentration weighted trajectory (CWT) sea salt source maps for southern Ecuador .

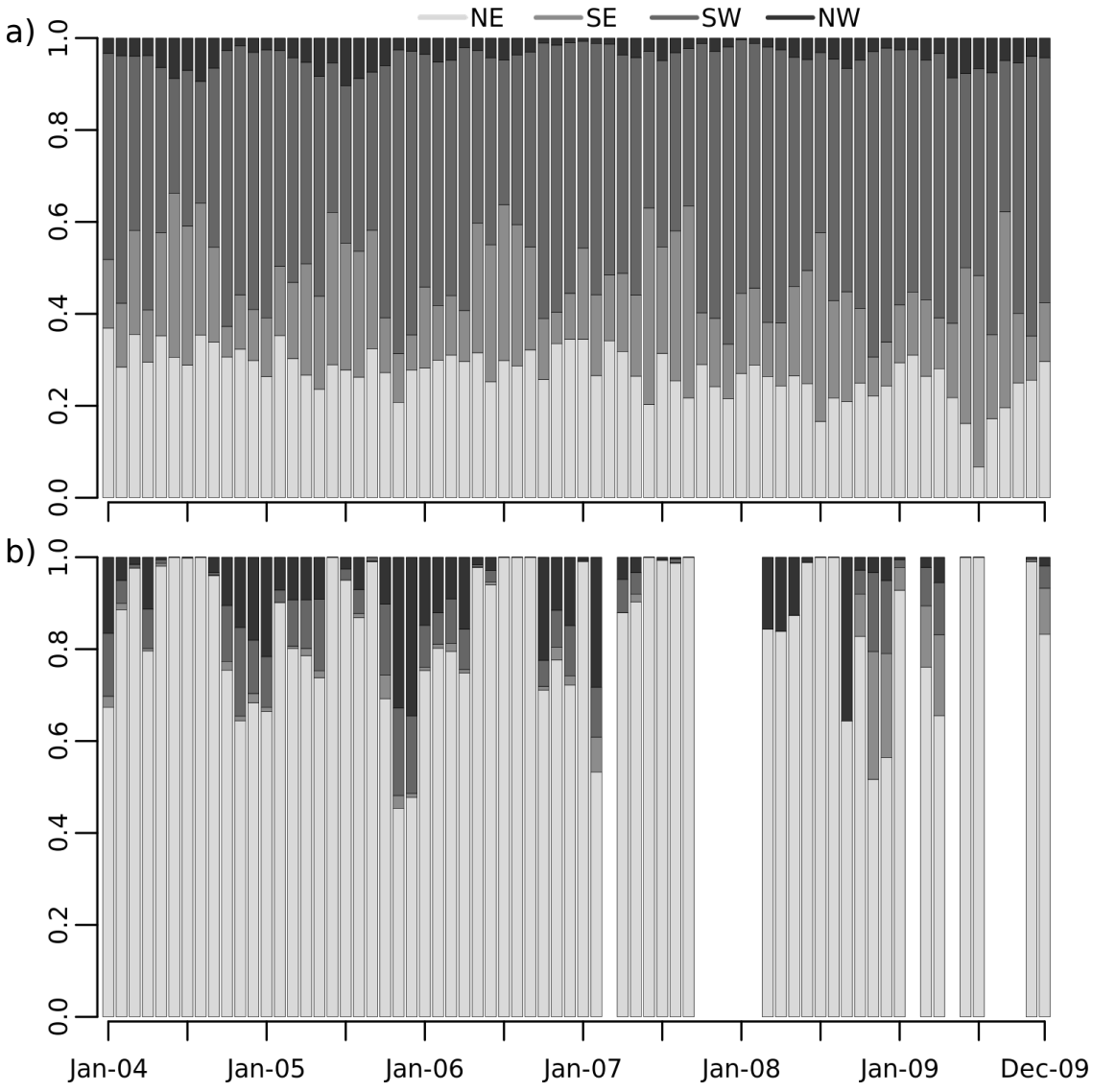

Figure 4. a Monthly wind sector relative frequency (%) Mean back-trajectories at 6000 m height level for the calculated clusters with origin at the *San Francisco* catchment in the Andes of south-eastern Ecuador meteorological stations a) ECSF and b) monthly time-series of sea-salt concentration from MACC reanalysis shown by the contribution of each cluster to the concentration *Cerro del Consuelo* .

As Fig.4 but for height level at 4200 m.

As Fig.4 but for height level at 3180 m.

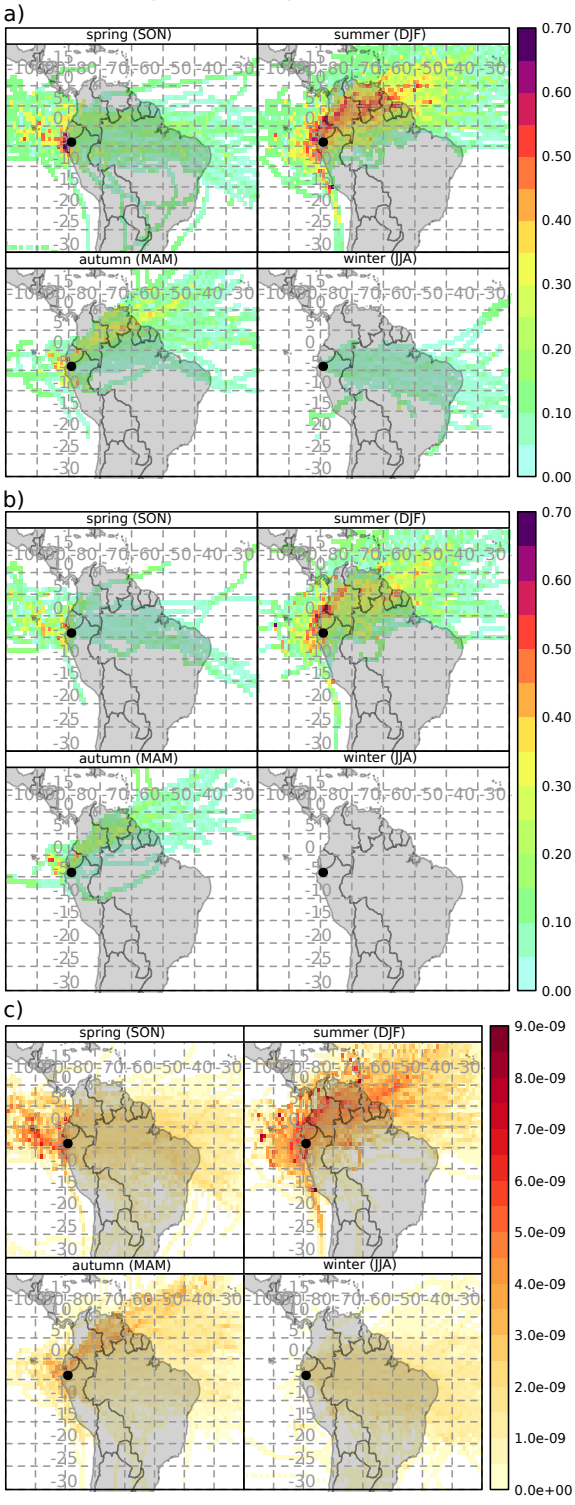

Figure 5. Potential Seasonal sea salt source maps according to a) potential source contribution function (PSCF) for (a with concentration threshold at 75th percentile , b,c) 75th and (d,e,f) PSCF with concentration threshold at 90th percentiles and (g,h percentile , i and c) concentration weighted trajectory (CWT)maps for ; the 2004-2009 period and three different back trajectory arrival starting height levels: 6000 m (left column), 4200 m (middle column), and is 3180 m at the receptor.

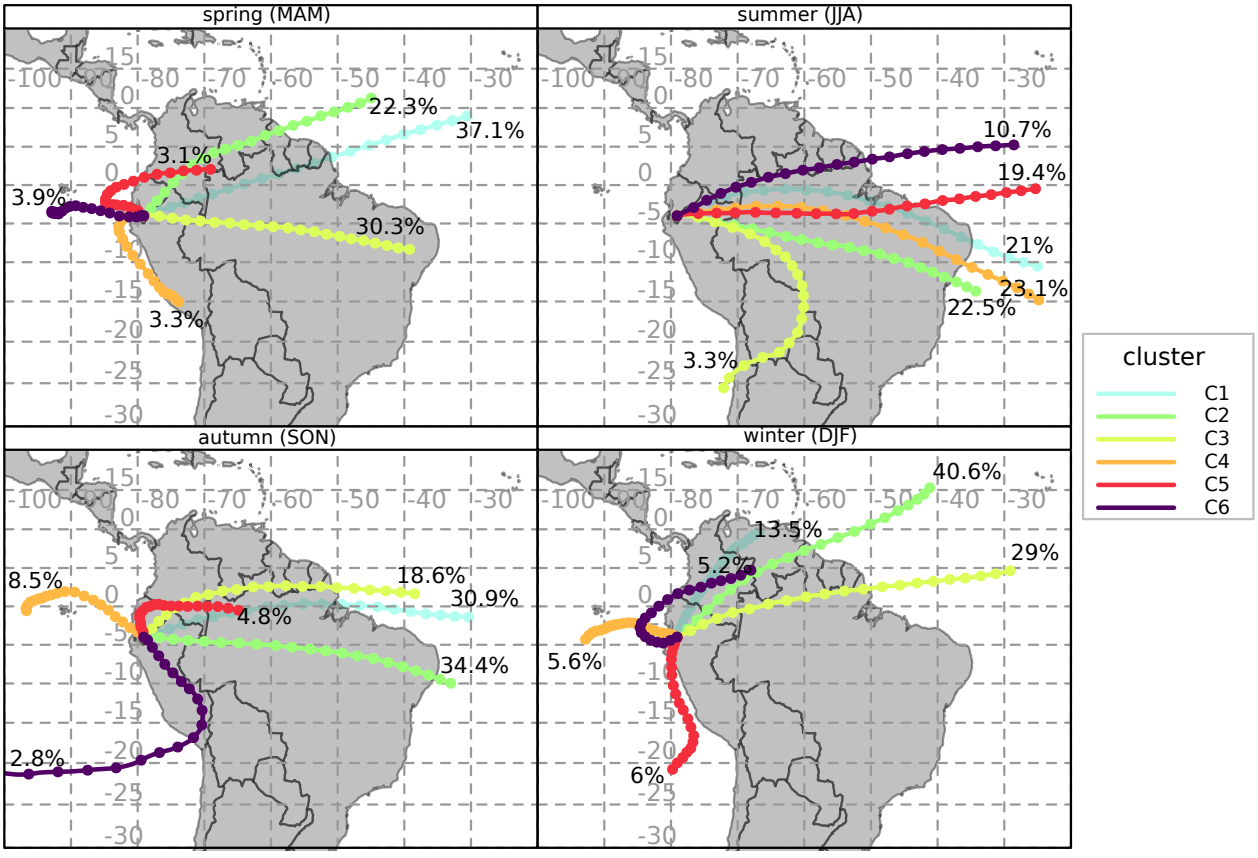

Figure 6. Seasonal mean back trajectory clusters (right column C1-C6).

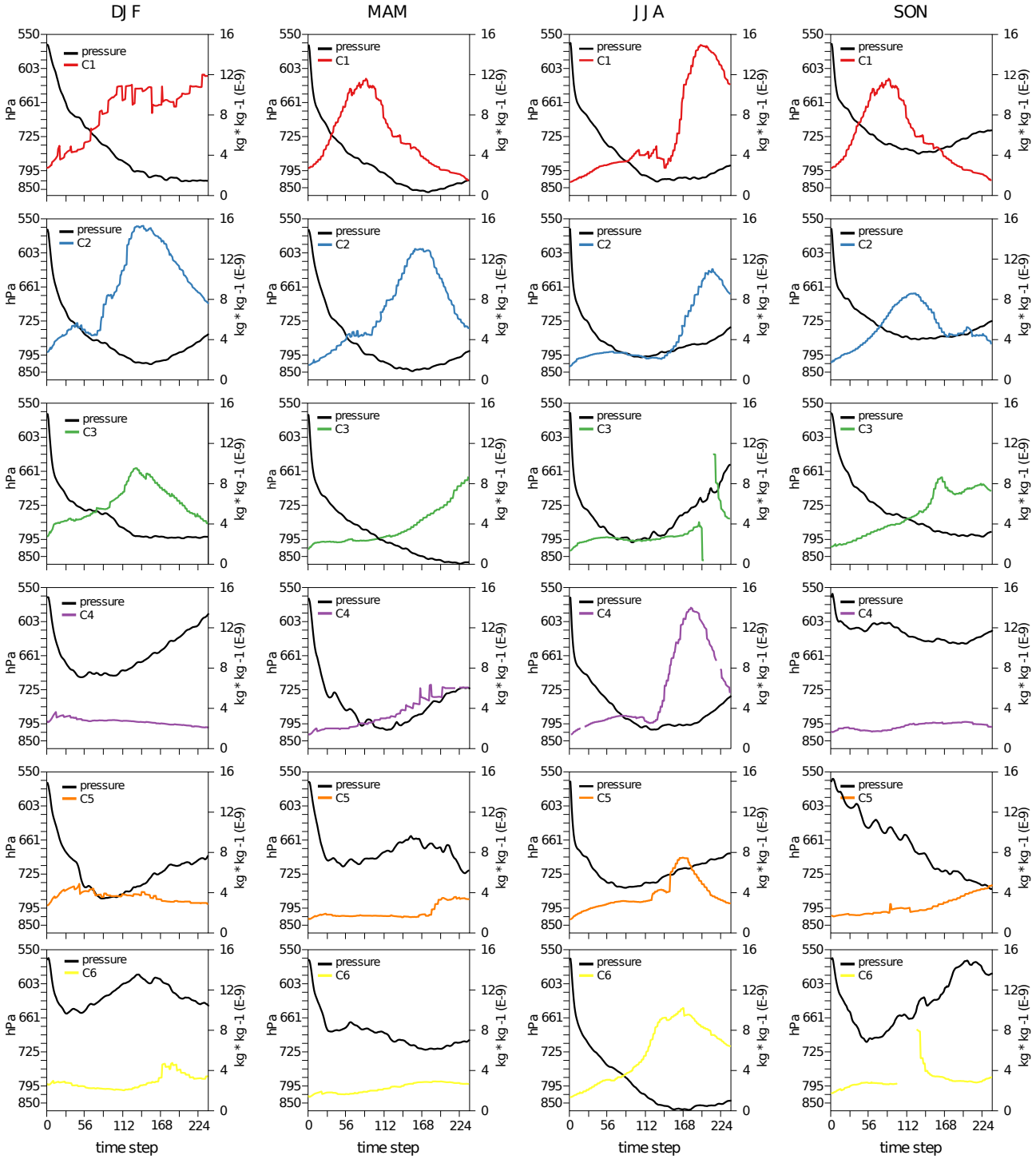

Figure 7. Seasonal plots of sea salt concentration and pressure level along mean back trajectory clusters. The colors of the sea salt concentration lines match those in the trajectory clusters in Fig. 6

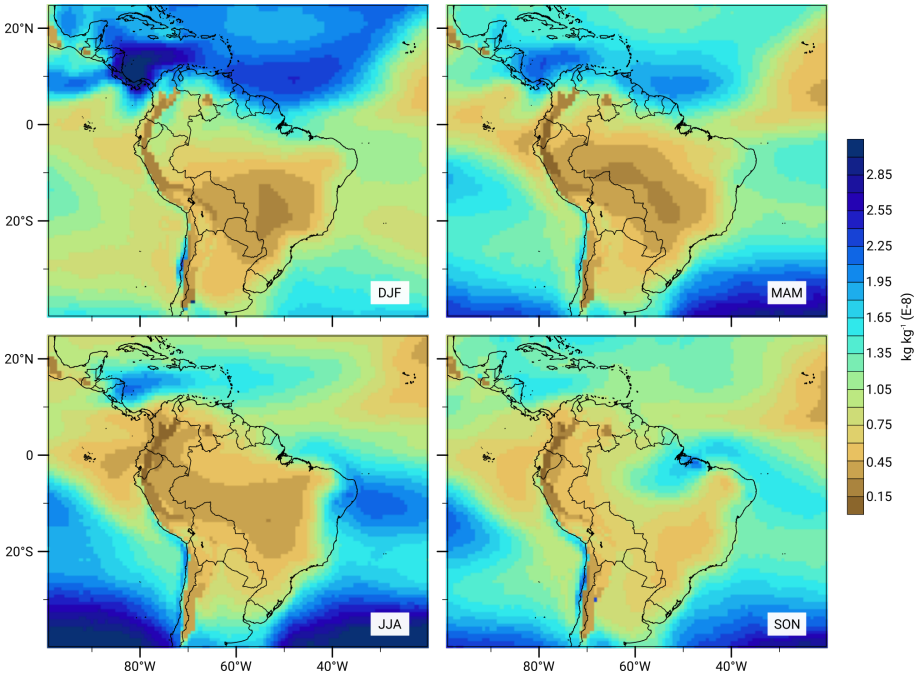

Figure 8. Sea Seasonal maps of sea salt concentration plotted by month (x axis) and year (y axis), and by cluster number for (A) 6000 m, (B) 4200 m, calculated from the Monitoring Atmospheric Composition and Climate (C MACC) 3180 m height level reanalysis model .

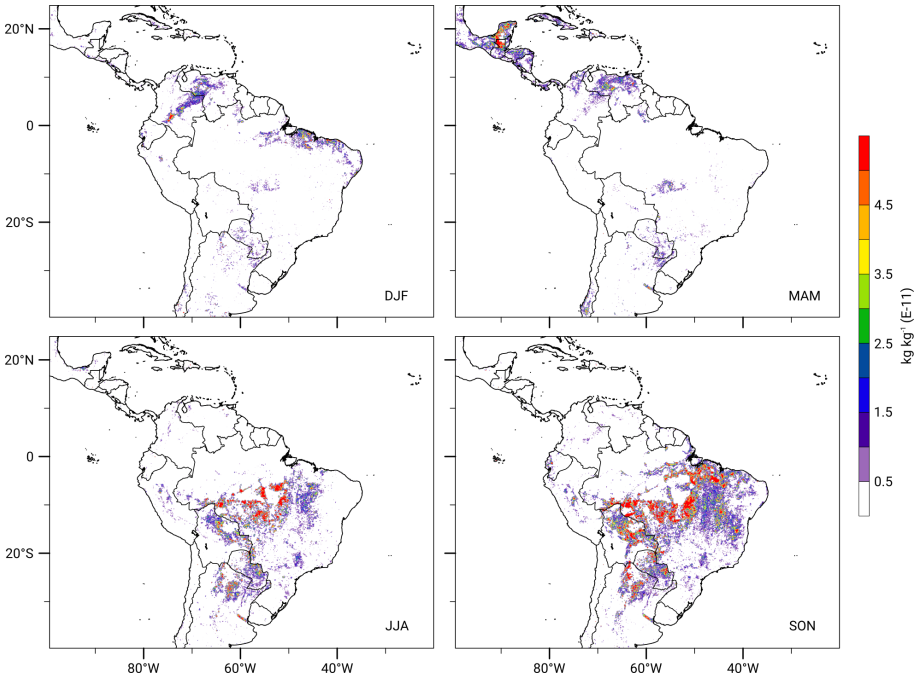

Figure 9. Maps Seasonal maps of seasonal potential source contribution function NO_x fluxes caused by biomass burning. Values were calculated from the Monitoring Atmospheric Composition and Climate (PSCF MACC) , 90th percentile concentration; trajectory arrival height level is 3180 m reanalysis model .

As Fig.9 but for concentration weighted trajectory (CWT).